How curtailment affects the spatial allocation of variable renewable electricity - What are the drivers and welfare effects?

AUTHOR

Dominic Lencz

EWI Working Paper, No 23/02

März 2023

Institute of Energy Economics at the University of Cologne (EWI)
www.ewi.uni-koeln.de

Institute of Energy Economics
at the University of Cologne (EWI)

Alte Wagenfabrik
Vogelsanger Str. 321a
50827 Köln
Germany

Tel.: +49 (0)221 277 29-100
Fax: +49 (0)221 277 29-400
www.ewi.uni-koeln.de

CORRESPONDING AUTHOR

Dominic Lencz
dominic.lencz@gmx.de

ISSN: 1862-3808

How curtailment affects the spatial allocation of variable renewable electricity - What are the drivers and welfare effects?

Dominic Lencz[a,*]

[a] *Institute of Energy Economics, University of Cologne, Vogelsanger Straße 321a, 50827 Cologne, Germany.*

Abstract

Variable renewable electricity (VRE), generated for instance by wind or solar power plants, is characterised by negligible variable costs and an availability that varies over time and space. Locating VRE capacity at sites with the highest average availability maximises the potential output. However, potential output must be curtailed, if system constraints prevent a local use or export. Such system constraints arise from the features defining the system, which I denote as system topology. Therefore, site choices that are unfavourable from a potential output perspective may still be optimal from a total system cost perspective. Previous research has shown that first-best investments require nodal prices that take account of the system constraints. Market designs that do not reflect nodal prices, such as uniform pricing, typically fail to achieve optimal site choices. However, a profound theoretical understanding of the economic trade-offs involved in the optimal spatial allocation of VRE is lacking. My paper contributes to filling this research gap. To do so, I develop a highly stylised model in which producers, taking into account the system topology, allocate VRE capacity in a one-shot game. Using the model, I analytically show that the optimal spatial allocation can be grouped into three spatial allocation ranges. Which of these ranges applies, I find to be highly dependent on the system topology parameters. In the first range, valid for relatively low VRE penetration levels, it is optimal to allocate all capacity to the node with the higher average availability. In the second and third range, it is optimal to allocate marginal capacity either fully or partially to the node with the lower average availability, i.e., the less favourable site from a potential output perspective. For uniform pricing, I show that producers allocate capacity inefficiently when VRE penetration exceeds a certain threshold. The resulting welfare losses I find to be especially high when transmission capacity is low, the difference in average VRE availability is large, and demand is concentrated at the node with the lower availability.

Keywords: variable renewable electricity, spatial allocation, nodal pricing, uniform pricing, theoretical analysis
JEL classification: Q42, Q48, D47

* *E-mail address*: dominic.lencz@gmx.de

1. Introduction

Variable renewable electricity (VRE), generated for instance by wind or solar power plants, is characterised by negligible variable costs. Another characteristic is that the availability of VRE sources is determined by external factors, such as wind speed or solar radiation, which vary over time and space. The product of the availability and the installed capacity defines the potential output. If the potential output can neither be used locally nor exported, it must be curtailed. Such electricity, which could be provided free of charge, cannot be used to generate welfare. In the year 2020, according to Yasuda et al. (2022), less than five per cent of the output of VRE was curtailed in most countries. However, curtailments are found to increase as VRE increases in several markets in Europe, America and Asia. In Ireland and Denmark, where VRE from wind already meets 35% and 45% of demand respectively, curtailment reaches 11% and 8% (Yasuda et al., 2022). The increase in curtailment is plausible because, as VRE penetration increases, VRE production more often exceeds demand and must be curtailed when it cannot be exported or stored. Sinn (2017), who extrapolates the German VRE penetration, finds that curtailment increases exponentially if no additional measures are taken. When the VRE share doubles from 30% to 60%, VRE curtailments are found to increase from zero to 16%. For a VRE share of 90%, more than 60% of total VRE output is curtailed in the analysis of Sinn (2017). In other words, meeting 90% of demand with VRE would require capacity with a potential output of more than 200% of demand. These figures highlight the increasing importance of curtailment in the context of VRE expansion.

To maximise welfare, curtailments should be reduced to an appropriate level: An appropriate level of curtailment balances the costs of curtailment and the costs of mitigating curtailment. The costs of curtailment arise from actions which compensate for the curtailed electricity, such as investing in additional VRE capacity. The costs of mitigating curtailment occur from actions which mitigate curtailment. Actions to mitigate curtailment are investments in storage and demand flexibility (e.g., Sinn, 2017; Zerrahn et al., 2018; Müller, 2017), network expansion (e.g., Fürsch et al., 2013), or a network-friendly allocation of VRE (e.g., Schmidt and Zinke, 2020). In this paper, I focus on the relationship between curtailment and the spatial allocation of VRE.

The spatial allocation decision when investing in VRE is driven by potential output. As the weather differs between sites, the potential output of VRE differs. Placing capacity at sites with the highest potential output maximises the potential output of VRE production. However, it is well known in the literature that system constraints may imply that unfavourable site choices from a potential output perspective may still be optimal

from a total system cost perspective (e.g., Schmidt and Zinke, 2020; Green, 2007; Obermüller, 2017; Pechan, 2017). The system constraints and their relevance are likely to depend on the features of the system. In the remainder of the text I denote the features of the system as system topology. For VRE, relevant parameters describing the system topology are the transmission capacity, the spatial distribution of demand, the VRE penetration, the correlation, the average and the variance of VRE availabilities, as well as the capacities of storage and demand flexibility. Similar observations regarding the effect of the spatial allocation on the total system costs apply to any investment in generation, storage, or demand (e.g., Green, 2007; Czock et al., 2022; Müller, 2017). Therefore, it has been shown that first best investments require nodal prices that take into account system constraints arising from the system topology (Schweppe et al., 1988). Vice-versa, it follows, and has been demonstrated in numerous case studies, that market designs which do not reflect nodal prices, such as uniform pricing, typically fail to identify optimal site choices (e.g., Schmidt and Zinke, 2020; Green, 2007; Obermüller, 2017; Pechan, 2017).

Against this backdrop, I shed more light on the impact of various parameters of the system topology on the spatial allocation of VRE in the social optimum and under uniform pricing. The existing literature lacks a comprehensive understanding of these issues. Instead, most papers analyse either the effect of single system topology parameters or the effect of the market design, i.e. nodal versus uniform pricing. In addition, most studies consider a specific real-world setting. For example, Elberg and Hagspiel (2015) analyse the effect of increasing VRE penetration on the market value of VRE for the case of Germany. The authors find that market values decrease most for regions with high availability, suggesting that for high VRE penetration it may be welfare enhancing to allocate some capacity to regions with moderate average availability. Schmidt and Zinke (2020) analyse the spatial allocation of wind capacity in Germany under nodal and uniform pricing for investments in the years 2020 to 2030. The authors find that 95% of the wind capacity added is allocated inefficiently, resulting in a welfare loss of 1.5% in terms of variable production costs. The most comprehensive analysis is provided by Pechan (2017). She analyses the impact of the correlation, the average and the variance of VRE availability on spatial allocation. She calculates the allocation in the social optimum and under uniform pricing and considers a 6-node network. Pechan (2017) finds that, under nodal pricing, producers increasingly concentrate capacity at high-availability nodes when the correlation increases and when the variance in the high-availability node is low. However, Pechan (2017) only analyses a setting where VRE serve 50% of demand, and she does not vary the transmission capacity or the demand distribution. She also performs a numerical analysis with few scenarios. Therefore, her results cannot be generalised.

To contribute to closing the research gap I analyse the following research questions:

1. From a theoretical perspective, under which states of the system topology is it welfare-enhancing to allocate some VRE capacity to sites with unfavourable potential output?
2. How does the spatial allocation differ between a uniform pricing regime and a first-best nodal pricing regime, and what are the resulting welfare effects?

To analyse these research questions, I develop a stylised theoretical model. The model depicts the spatial allocation of VRE sources in a two-node network with limited transmission capacity. At the two nodes consumers have a constant demand that must be satisfied by producers who can use a conventional and a VRE technology. The central element of the model is that producers decide how to spatially allocate VRE capacity. I model the spatial allocation of all VRE capacity as a one-shot game where producers consider a specific system topology, i.e. one specific configuration of transmission capacity, spatial distribution of demand, VRE penetration and VRE availability. This differs from reality, where VRE penetration other system topology parameters dynamically evolve over time. The implications from assuming a one-shot game I discuss in Section 5. The model considers availabilities which vary over time and between the nodes. The temporal sequence of availabilities I refer to as availability profile. The average availability I assume to be higher in one node (i.e. high-availability node) compared to the other node (i.e. low-availability node). The effect of storage and demand flexibility I do not analyse in the model itself to ensure an analytical solution. The analytical solution is crucial to gain a profound theoretical understanding. To still shed light on the effect of storage and demand flexibility, I discuss the effects qualitatively based on the model results and findings from other papers in Section 5. To analyse the relationship between spatial allocation under a first-best nodal pricing regime and a uniform pricing regime, I solve the model for both market designs.

The main findings of the analysis regarding the first research question are as follows: The optimal spatial allocation can be grouped into three spatial allocation ranges that are valid for different levels of VRE penetration. For a low levels of VRE penetration, all VRE capacity should be allocated to the high-availability node (i.e. *high-availability deployment range*). For such levels of VRE penetration, it is not welfare enhancing to allocate some VRE capacity to sites with unfavourable potential output. For a higher levels of VRE penetration, resulting in curtailments that completely eliminate the advantage arising from a higher average availability, it is optimal to allocate the additional capacity only to the low-availability node (i.e. *low-availability deployment range*). This is because the additional capacity would increase the marginal curtailments at the high-availability node, while small capacities at the low-availability node do not need to

be curtailed. For an even higher levels of VRE penetration, resulting in curtailments at the low-availability node, it is optimal for producers to split additional capacity between the two nodes (i.e. *split capacity deployment range*). Thus, at higher levels of VRE penetration, it is welfare enhancing to allocate (some) VRE capacity to less favourable sites from the perspective of potential output. The VRE penetration levels, which mark the cut-off points between the three ranges, I derive analytically. The results imply, that the cut-off points depend on the parameter configuration of the system topology.

Therefore, the width of the *high* and *low-availability deployment range* and the capacity split under the *split capacity deployment range* are affected by the system topology. Increasing the transmission capacity and demand share at the high-availability node widens the *high-availability deployment range* and narrows the *low-availability deployment range*. In the *split capacity deployment range*, more capacity is allocated to the high-availability node. A higher correlation between the nodal availability profiles increases the share of capacity allocated to the high-availability node in the *split capacity deployment range*. Higher availabilities at the low-availability node narrow the *high-availability deployment range* so that the overall share of VRE allocated to the low-availability node increases. The impact of nodal availability profiles is found to be influenced by transmission capacity. In the case of correlation, the impact of changes in correlation increases with increasing transmission capacity. The direction of the effect of changes in the availability and variance in the *split capacity deployment range* even depends on the transmission capacity. Increasing the average and decreasing the variance of the nodal availability increases the nodal share when the transmission capacity is high. The opposite happens when the transmission capacity is low. Therefore, the availability profiles alone are not sufficient to indicate the optimal spatial allocation, but need to be considered in combination with the level of transmission capacity.

Regarding the second research question, my analysis provides the following insights: Under uniform pricing, producers allocate capacity only to the high-availability node for higher VRE penetration levels than socially optimal. This is because network constraints that would induce producers to allocate capacity more in line with demand are ignored. Welfare losses occur when marginal curtailments due to limited transmission capacity exceed the average availability advantage of the high-availability node. Welfare losses increase with increasing VRE penetration until VRE penetration is sufficiently high that differences in availability profiles provide an incentive to allocate some capacity to the low-availability node. Welfare losses under uniform pricing decrease with the level of transmission capacity and increase with the need for transmission.

From a theoretical perspective, my contribution is threefold: First, using a highly stylised model, I show that the optimal spatial allocation can be grouped into three ranges. I analytically derive the VRE penetration levels that separate the three ranges, so that the results can be applied to any feasible configuration of the system topology. Second, I identify the effect of various parameters of the system topology on the optimal spatial allocation of the ranges. And third, I identify the allocation under uniform pricing and the resulting welfare loss, and show how the welfare loss is affected by the different parameters of the system topology.
Due to my model's simplicity I analyse a highly stylised setting. When analysing a more realistic setting additional effects will occur. Such effects from considering a more realistic setting on my theoretical findings are discussed in Section 5. Combining the findings from the theoretical analysis with the considerations from the discussion can help policymakers when designing policies that affect the spatial allocation or when considering a change in the market design. Investors can use the results when trying to find the profit-maximising allocation of VRE investments.

2. Model

I develop a theoretical model to analyse the effect of the VRE penetration, the transmission capacity, the demand distribution, the VRE availabilities, and the market design on the spatial allocation. The effect of storage and demand flexibility I do not analyse in the model itself to ensure an analytical solution. To shed light on the effect of storage and demand flexibility, I discuss the effects qualitatively based on the model results and findings from other papers in Section 5.
The model considers the interaction between profit-maximising producers in a perfectly competitive environment, consumers, and a regulator. The players act in a network consisting of two nodes, h and l (i.e., $i \in (h, l)$), which are connected by a transmission line with the transmission capacity t. Furthermore, I define the model to have three stages, the regulation stage (τ_1), the spatial allocation stage (τ_2), and the market clearing stage (τ_3). As the model is solved by backward induction, the explanation starts with the last stage. In the market clearing stage (τ_3), the consumers at both nodes have a constant and inelastic demand over a continuous time interval ranging from 0 to 1 (i.e., $\int_0^1 d_i \, dx = d_i$). I assume the nodal demand to exceed the transmission capacity (i.e., $d_i > t$). I also assume that the producers can satisfy the demand with one conventional and one VRE technology. This assumption differs from the situation in most countries, where several conventional and at least two VRE technologies, namely wind and solar, are employed. On the one hand, the assumption of one conventional and one VRE technology allows to derive the effect of the spatial allocation of VRE analytically. This provides a general understanding of the impact of the system topology.

On the other hand, the simplification of multiple production technologies into one conventional and one VRE technology highlights the stylised nature of the model. The implications of this simplification are discussed in Section 5. The conventional technology induces constant marginal production costs of c when producing one unit of output[1]. I assume the conventional capacity at nodes h and l to exceed the respective demands. As the producers operate in a competitive environment, they cannot charge prices above the marginal costs c of the conventional technology. Therefore, producers cannot make profits by investing in the conventional technology and have no incentive to invest in this technology.[2]

The VRE technology induces zero marginal costs. However, the total installed capacity is limited to v. The capacity at node h and l is represented by V_h and $V_l = v - V_h$. The VRE capacity cannot always produce at full capacity, but only at the availability ($avail_i$) times the installed capacity (I_i). Availability varies over time and between the nodes ($avail_i$). The temporal sequence of availabilities I refer to as availability profile ($AVAIL_i(\mu_i, \sigma_i^2)$). The availability profile at each node is characterised by the average availability (μ_i) and the variance (σ_i^2). I assume the availability profile to be beta distributed (i.e., $B(\alpha_i, \beta_i)$). The beta distribution is chosen because it has positive densities only for values in the interval $[0, 1]$, as VRE availabilities do in reality. Furthermore, choosing the parameters α_i and β_i appropriately, results in density functions similar to those of wind or solar power plants, as shown in Appendix Appendix A. In addition, relevant statistical moments can be calculated based on the parameters α_i and β_i. The average availability is given by $\mu_i = \frac{\alpha_i}{\alpha_i+\beta_i}$ and the variance is defined by $\sigma_i^2 = \frac{\alpha_i\beta_i}{(\alpha_i+\beta_i+1)(\alpha_i+\beta_i)^2}$.[3] The product of the average availability and the installed capacity defines the potential output (PO_i):

$$PO_i = \mu_i I_i \tag{1}$$

I assume $\mu_h > \mu_l$, so that I call node h as *high-availability node* and node l as *low-availability node*. The availabilities at the two nodes can be correlated, with $\rho_{h,l} \in [-1, 1]$ being the correlation coefficient. Highly correlated availabilities (i.e., $\rho_{h,l}$ close to 1) imply that a high availability in h tends to coincide with a high availability in l and vice versa. If the availabilities are barely correlated (i.e., $\rho_{h,l}$ close to 0), high availabilities in h are similarly likely to be accompanied by high or low availabilities in l. The potential output resulting from the capacities times the availabilities that can neither be consumed locally nor be

[1]These costs include fuel costs as well as other all relevant variable costs such as costs for carbon emission allowances.

[2]In reality, investment in conventional capacity can be observed. There are two main reasons for this. First, conventional capacity often does not exceed demand, so that producers can make profits by offering capacity in periods of scarcity. Such scarcity tends to persist as older plants are retired. Second, the marginal cost of building new conventional technologies tends to fall over time, so that new capacity can be profitable even in the absence of scarcity.

[3]Both parameters, α and β, affect the average and the variance simultaneously. However, for $\mu_i \in [0.2, 0.4]$, increasing α_i primarily increases μ_i, while σ_i is barely affected. A numerical example showing these effects I provide in Appendix C.

exported is curtailed. I define the sum of nodal curtailment as C_i and the difference between the potential output (PO_i) and C_i as usable output (UO_i):

$$UO_i = PO_i - C_i \tag{2}$$

In the spatial allocation stage (τ_2), the producers allocate the VRE capacity between nodes h and l. The respective capacities I define as V_h and $V_l = v - V_h$. I model the spatial allocation of all VRE capacity as a one-shot game where producers consider a particular system topology, i.e. transmission capacity, spatial distribution of demand, VRE penetration and VRE availability. This differs from reality, where VRE penetration increases continuously and other system topology parameters also evolve dynamically. The implications of assuming a one-shot game I discuss in Section 5. Producers choose the allocation between h and l such that their profits are maximised. When deciding on the spatial allocation, the producers have perfect foresight, i.e., they know the nodal demand and the nodal availability profiles. In addition, producers take into account the underlying market design as well as the total level of VRE capacity, which I denote by v. All parameters presented, namely the demand (d_i), the transmission capacity (t), the VRE penetration (v), and the parameters determining the nodal availability profiles (μ_i, σ_i, $\rho_{h,l}$) define the system topology.

In this paper I focus on the optimal spatial allocation of VRE and not on the optimal capacity (v). Therefore, I assume that the regulator defines the total VRE capacity in the regulation stage (τ_1).[4]
In addition, the regulator defines the market design. The market design options the regulator can implement are nodal and uniform pricing. Under nodal pricing the nodal demand and supply define the nodal price, considering the network transmission capacity. The prices at both nodes may differ, as shown in the following example: Assume the potential VRE output at node h exceeds the nodal demand plus the transmission capacity ($PO_h > d_h + t$). In that case, some VRE at node h needs to be curtailed, and the VRE technology sets the nodal price. As the VRE technology feature zero marginal costs the price at node h is zero (i.e.,$p_h = 0$). At the same time, the potential VRE output at node l plus the VRE imports from node h are below the demand in l (i.e., $PO_l < d_l - t$). As a result, some conventional output is required to satisfy the demand at node l, such that the conventional technology sets the price (i.e., $p_l = c$). Depending on the system topology, the price at both nodes will be c in some situations and 0 in others. The proportion of

[4]To identify the optimal v in the model at hand one would have to consider the capital costs of the VRE technology and to minimise the total costs with respect to the total VRE capacity; When the regulator defines v, she may use auctions which allow for negative prices and contain an obligation to build the purchased capacity. Such a process would ensure the total capacity is sold in this stage, built and allocated in the spatial allocation stage and used in the market clearing stage.

situations where the conventional technology sets the price represents the average nodal price $\overline{p_i}$.

Under uniform pricing, the price producers receive is determined by the global demand ($d_h + d_l = d_{h+l}$) and supply. Thus, the market design implicitly ignores transmission constraints and yields identical prices at both nodes (i.e., $p_h = p_l$). The conventional technology sets the price (i.e., $p_i = c$) when the global demand exceeds the global VRE potential. When the global VRE potential exceeds the global demand, the VRE technology sets the price (i.e., $p_i = 0$). The proportion of situations where the conventional technology sets the price represents the average price $\overline{p_i}$. Under uniform pricing, situations may arise where output sold with VRE production cannot be dispatched to the consumers due to limited transmission capacity. I assume such VRE output is curtailed, but producers still receive the market price. This is similar to the compensation applied in multiple countries with uniform pricing, such as, for instance, Germany, Denmark, Italy or Japan (Bird et al., 2016). To ensure demand is met, the curtailed VRE production is replaced by additional conventional production at the other node. Such conventional production I denote by redispatch. These costs are assumed to be borne by the consumers. Figure 1 schematically represents the model setup including the three stages.

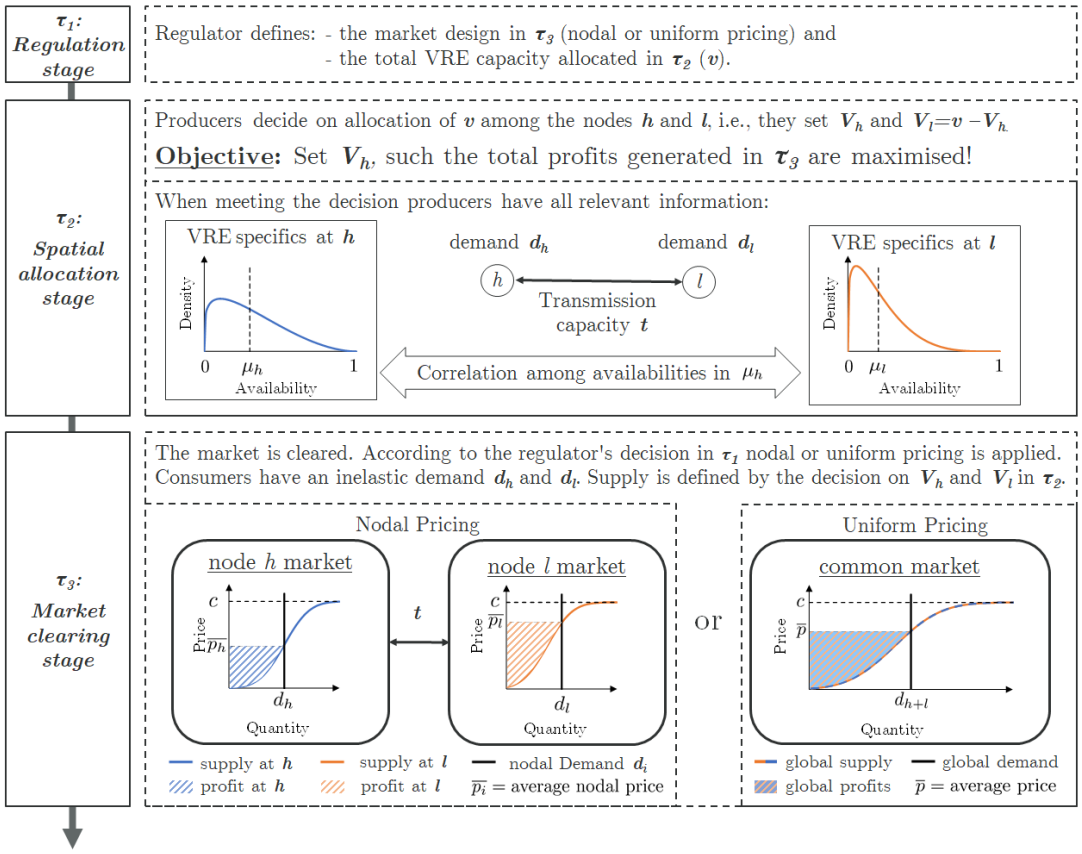

Figure 1: Schematic representation of the model setup.

3. Spatial allocation under nodal pricing

In this section I analyse the socially optimal spatial allocation under nodal pricing. To do so, I first derive the spatial allocation rationale of producers facing such a market design. As the spatial allocation differs depending on the level of VRE penetration, the ranges in which capacity allocation can be grouped are identified. In a last step, the effect of transmission capacity, demand distribution, and VRE availability profiles on the width of the ranges and spatial allocation within the ranges are assessed. Thereby the interactions among the parameters are considered.

3.1. Spatial allocation rationale

Based on the analysis of the producers' rationale when spatially allocating VRE capacity under nodal pricing, perfect competition and perfect foresight, I conclude that:

Finding NP 1. *Under nodal pricing, producers aim to allocate the capacity such that the marginal usable output is identical at both nodes. If marginal usable outputs differ independent of the capacity allocation, producers allocate all capacity to the node with higher marginal usable output.*

Explanation. Under nodal pricing, perfect competition and perfect information, the producers' maximisation of profits coincide with the minimisation of the total costs (TC). Hence, producers spatially allocate the capacity such that the total costs are minimised. Within the total costs, the capacity level in l (V_l) can be substituted with $v - V_h$, such that V_h is the only decision variable. The total costs are given by the product of conventional production times their marginal costs (c). The level of conventional production is given by the sum of demand (d_{l+h}) minus the sum of usable output ($\sum_i UO_i$) generated by VRE capacity. The usable output is defined by the difference between potential output (PO_i) and curtailment (K_i). Hence, total costs are given by:

$$\min_{V_h} \; TC = \left(\int_0^1 \underbrace{d_{h+l}}_{\text{demand}} - \underbrace{\left(\sum_i PO_i(V_h) \sum_i K_i(V_h) \right)}_{\text{usable output}} \right) c \tag{3}$$

The cost minimisation problem is solved by taking the derivative of Equation 3 with respect to V_h and equate the term to zero. Restructuring and resubstituting $v - V_h$ with V_l yields the following equilibrium:

$$\underbrace{\frac{\partial PO_h}{\partial V_h}}_{\substack{\text{marginal} \\ \text{potential in } h}} - \underbrace{\frac{\partial C_h}{\partial V_h}}_{\substack{\text{marginal} \\ \text{curtailment in } h}} = \underbrace{\frac{\partial PO_l}{\partial V_l}}_{\substack{\text{marginal} \\ \text{potential in } l}} - \underbrace{\frac{\partial C_l}{\partial V_l}}_{\substack{\text{marginal} \\ \text{curtailment in } l}} \tag{4}$$

Hence, the spatial allocation rationale, which maximises the producers' profits, is to allocate capacity such that the marginal potential output minus marginal curtailment is identical at both nodes. The difference between marginal potential output and marginal curtailment describes the marginal usable output. Marginal output is usable when the nodal demand exceeds the sum of nodal potential output and potential VRE imports.

$$\frac{\partial UO_i}{\partial V_i} = \frac{\partial PO_i}{\partial V_i} - \frac{\partial K_i}{\partial V_i} \tag{5}$$

As described in Section 2 the price in situations when the marginal output is usable is set by the marginal costs of the conventional technology, c. Therefore, the marginal usable output time c represent the marginal profit:

$$\frac{\partial \text{Profit}_i}{\partial V_i} = \frac{\partial UO_i}{\partial V_i} c \tag{6}$$

Hence, producers maximise their profits by allocating the VRE capacity such that the marginal profit is identical at both nodes.

The finding can be explained as follows: Producers aim to maximise their profits by optimising their VRE capacity allocation. If marginal profits differ between the nodes, producers allocate more capacity to the node with higher marginal profits. This results in increased nodal curtailment and decreased nodal profit as average prices decrease. Producers continue the process until the marginal profits are identical at both nodes. At such an allocation, the marginal usable output is identical at both nodes.

If Equation 4 does not hold for any permissible spatial allocation (i.e., $V_h \in (0, v)$), producers maximise their profits by allocating all capacity to the node, that offers higher marginal profits. This node also features higher marginal usable output, according to Equation 6.

End of Explanation.

When plugging the Beta distribution into the objective function, most elements of the described derivatives can be calculated. The marginal potential output is given by the average output of one capacity unit:

$$\frac{\partial PO_i}{\partial V_i} = \mu_i = \frac{\alpha_i}{\alpha_i + \beta_i} \tag{7}$$

Curtailment, K_i, arises from limited transmission capacity (K_i^t) and when the VRE potential exceeds global demand (K_i^d).

$$K_i = K_i^t + K_i^d \tag{8}$$

K_i^t occurs when the nodal VRE potential exceeds the nodal VRE demand plus the transmission capacity $(d_i + t)$. The curtailment is defined by V_i times the availability minus $d_i + t$. As the availabilities are not constant over time, the availability density function $B(\alpha_i, \beta_i)$ has to be considered when the integral of curtailment is calculated. The integral ranges from $[\frac{d_i+t}{V_i}; 1]$ because only if availabilities are larger than $\frac{d_i+t}{V_i}$ output is curtailed due to limited transmission capacity and availabilities cannot exceed 1. As a result, the level of curtailment is defined by the following integral:

$$K_i^t(V_i) = \int_{\frac{d_i+t}{V_i}}^{1} \underbrace{(x - \frac{(d_i+t)}{V_i})V_i}_{\text{level of curtailment}} \underbrace{\frac{1}{B(\alpha_i, \beta_i)} x^{\alpha_i - 1}(1-x)^{\beta_i - 1}}_{\text{availability density}} dx \qquad \text{if } V_i > d_i + t \tag{9}$$

By integrating Equation 9 the level of curtailment can be rewritten as:

$$\frac{\alpha_i}{\alpha_i + \beta_i} V_i + \frac{(d_i+t) B_{\frac{d_i+t}{V_i}}(\alpha_i, \beta_i) - V_i B_{\frac{d_i+t}{V_i}}(1+\alpha_i, \beta_i)}{B(\alpha_i, \beta_i)} - (d_i + t) \tag{10}$$

The marginal curtailment due to limited transmission capacity arising from an additional unit of V_i is given the taking the derivative with respect to V_i:

$$\frac{\partial K_i^t(V_i)}{\partial V_i} = \frac{\alpha_i}{\alpha_i + \beta_i} - \frac{B_{\frac{d_i+t}{V_i}}(\alpha_i + 1, \beta_i)}{B(\alpha_i, \beta_i)} \tag{11}$$

The curtailment arising when VRE potential exceeds global demand depends on the joint distribution of the availabilities of the nodes h and l. The joint distribution depends on the specific beta distribution parameter α_i, β_i, the correlation $\rho_{h,l}$, as well as the nodal demands d_i. The curtailment arising when demand exceeds the global demand and its marginal cannot be derived analytically in a universal manner. The values are calculated numerically in the following subsections.

3.2. Capacity allocation ranges

In this subsection, I derive the capacity allocation ranges which occur based on the spatial allocation rationale stated in the previous subsection. I conclude that:

Finding NP 2. *The optimal spatial allocation can be grouped into three spatial allocation ranges which are valid for different level of VRE penetration. For low VRE penetration levels, producers allocate capacity to the high-availability node (high-availability deployment range). For higher VRE penetration levels, producers allocate capacity to the low-availability node (low-availability deployment range), and for even higher VRE*

penetration levels, producers split the capacity among the two nodes (split capacity deployment range).

Explanation. For low VRE penetration levels, producers allocate capacity to the high-availability node, which I denote as *high-availability deployment range*. This can be explained as follows: For $V_i < d_i$, curtailment is absent, such that marginal usable output coincides with marginal potential output to both nodes. To maximise profits, producers allocate capacity to the node with the higher average availability (i.e., node h). When V_h exceeds $d_h + t$ curtailment occurs.[5] The curtailment increases with increasing V_h, as the second derivative of the curtailment arising from limited transmission capacity (Equation 11) with respect to V_h is positive:

$$\frac{\partial^2 K_h^t}{\partial V_h^2} = \frac{(\frac{d_h+t}{V_h})^{1+\alpha_h}(1-\frac{d_h+t}{V_h})^{-1+\beta_h}}{V_h B(\alpha_h,\beta_h)} > 0 \quad \text{for: } \alpha_h > 0,\ \beta_h > 0,\ d_h > 0,\ v > V_h,\ V_h > d_h + t \tag{12}$$

As long as the marginal usable output at node h (i.e., $\frac{\partial PO_h}{\partial V_h} - \frac{\partial \overline{C}_h}{\partial V_h}$) exceeds the marginal potential output at node l (i.e., $\frac{\partial PO_l}{\partial V_l}$), producers allocate the capacity solely to the high-availability node. When those values are identical the *high-availability deployment range* ends. The VRE penetration level which marks the cut-off point between the *high-availability deployment range* and the *low-availability deployment range* I denote by $v^{H|L}$:

$$v^{H|L} = V_h[\mu_h - \frac{\partial K_h^t}{\partial V_h} - \mu_l = 0] \tag{13}$$

Producers allocate additional capacity in the *low-availability deployment range* to node l, because for low VRE penetration at node l curtailments at this node are absent, such that marginal usable output is not affected by an increase in V_l. Allocating additional capacity to node h would increase marginal curtailment, resulting in lower marginal usable output. Producers solely place additional capacity to node l until curtailment occurs. By assuming $\rho_{h,l} > -1$, there is a positive probability that the highest possible output at node l (i.e., $avail_l = 1$) coincides with a potential output at node h exceeding $d_h + t$, i.e., $P(avail_l = 1 | PO_h \geq d_h + t) > 0$. Hence, curtailment at node l occurs when V_l exceeds $d_l - t$. The VRE penetration level which marks the cut-off point between the *low-availability deployment range* and the *split capacity deployment range* I denote by $v^{L|S}$:

$$v^{L|S} = v^H + (d_l - t) \tag{14}$$

When curtailment occurs at node l, producers split additional capacity among the two nodes. The range I denote as *split capacity deployment range*. Producers split the capacity because curtailment decreases the

[5] Due to the absence of VRE production at node l and $t < d_l$ there is no curtailment due to limited import ability from node l.

marginal usable output at both nodes. To maximise the profits, producers split additional capacity such that the marginal usable output is identical at both nodes. The split of nodal capacity depend on the transmission capacity, the demand distribution, and the VRE availability profiles, which are analysed in the following subsections.

End of Explanation.

Figure 2 demonstrates the insights from Finding NP 2 numerically. The availability density parameters are chosen to resemble the availabilities for wind in the north (h) and south (l) of Germany. A comparison of the assumed and the historical German availability density for wind power is presented in Appendix B. The demand is split equally among the nodes, and the transmission capacity can transmit one-fourth of the nodal demand. The orange line in the upper diagram displays the marginal capacity share allocated to node h. A value of 1 indicates that producers allocate additional capacity units to node h. A value of 0 indicates the marginal capacity unit is allocated to node l. Values in between imply that producers split marginal capacity among the two nodes.

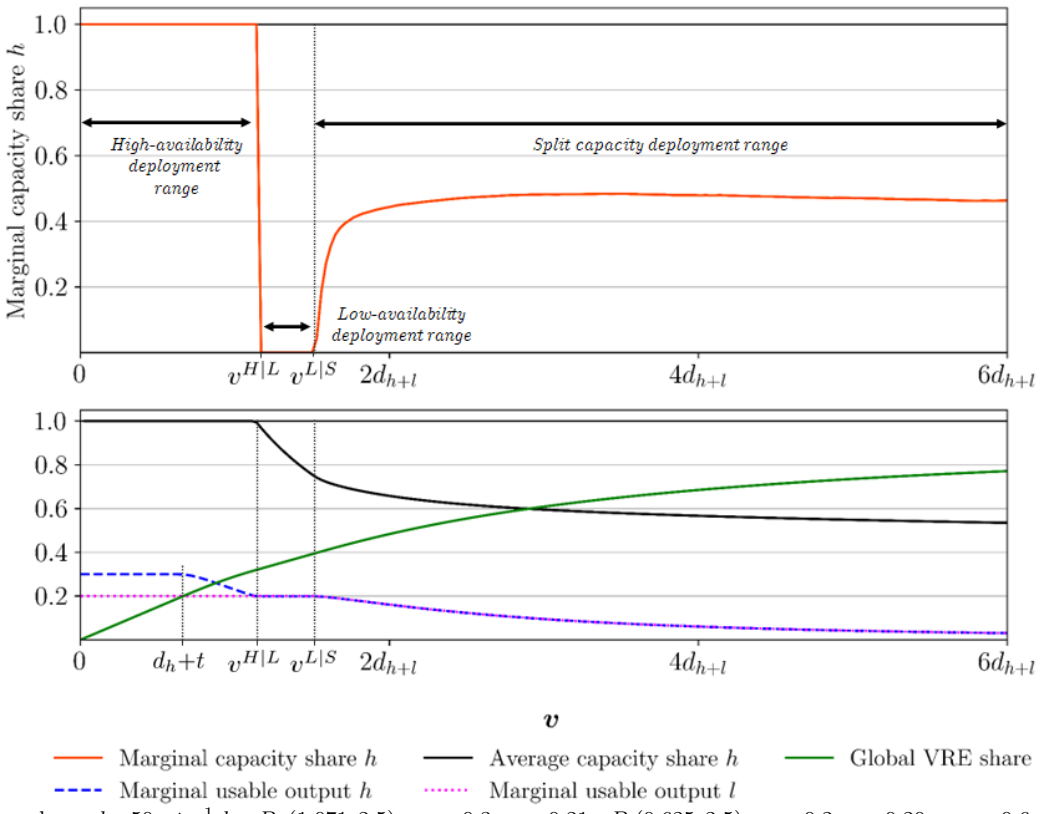

Parameter values: d_i=50, t=$\frac{1}{4}d_i$, $B_h(1.071, 2.5)\rightarrow\mu_h$=0.3, σ_h=0.21, $B_l(0.625, 2.5)\rightarrow\mu_l$=0.2, σ_l=0.20, $\rho_{h,l}$=0.6.

X-axis values: $v^{H|L} = 1.1d_{h+l}$ and $v^{L|S} = 1.1d_{h+l} + (d_l - t)$.

Figure 2: Spatial allocation, marginal usable output, and VRE share at different VRE penetration levels under nodal pricing.

For low levels of VRE penetration, all capacity is allocated to node h (i.e., *high-availability deployment range*). For $v < d_h + t$ curtailment is absent. For $v = d_h + t$, VRE supplies roughly 20% of the demand. For higher VRE capacity levels, marginal curtailment is higher such that the marginally usable output is lower. For $V^h = v^{H|L} = 1.1d_{h+l}$, the marginal usable output is identical at both nodes, and the *high-availability deployment range* ends. At this point, VRE supplies 33% of the demand.

When VRE levels range between 33-40%, capacity is allocated solely to node l. The VRE penetration marking the shift from the *low-availability deployment range* to the *split capacity deployment range* is given by $v = v^{L|S} = 1.1d_{h+l} + (d_l - h)$. At this VRE penetration level $V_l = d_l - l$ holds. For higher VRE shares, the capacity is split among the nodes. For VRE levels above 50%, producers allocate roughly half of the capacity to each node.

Based on these observations, the question arises of how the transmission capacity, demand distribution, and availability profiles affect the capacity allocation ranges.

Additionally, the figure highlights the relevance of curtailment with increasing VRE penetration. At $v = 6d_{h+l}$, the potential output exceeds 1.5 times the global demand. However, the VRE share remains below 80%. This is because roughly 50% of VRE output is curtailed (not shown in the figure). The marginal curtailment at such a high VRE penetration level even reaches 85% at node l and 90% at node h (not shown in the figure).

3.3. Effect of changes in the transmission capacity

In this subsection, I derive the effect of changes in the transmission capacity (t) on the width of the capacity allocation ranges and the capacity split in the *split capacity deployment range*. Thereby the assumption $t < d_i$ (stated in Section 2) is relaxed. Based on the analysis, I conclude:

Finding NP 3. *Under nodal pricing, increasing the transmission capacity t widens the high-availability deployment range and narrows the low-availability deployment range. For $t \geq d_l$, the low-availability deployment range disappears. In the split capacity deployment range, the share of the high-availability node increases with increasing t.*

Explanation. Increasing the transmission capacity widens the *high-availability deployment range* as Producers are willing to allocate capacity solely to the high-availability node for higher VRE penetration levels. This arises due to two effects: First, when increasing t by one unit, it is possible additional capacity unit at node h without inducing curtailments. Second, the marginal curtailment arising from limited transmission capacity decreases with increasing t. This is the case as the derivative of $\frac{\partial K_h^t}{\partial V_h}$ (i.e., Equation 11) with respect to t is

negative:

$$\frac{\partial^2 K_h^t}{\partial V_h \partial_t} = -\frac{(\frac{d_h+t}{V_h})^{\alpha_h}(1-\frac{d_h+t}{V_h})^{-1+\beta_h}}{V_h B(\alpha_h,\beta_h)} < 0 \quad \text{for: } \alpha_h > 0,\ \beta_h > 0,\ \ d_h > t \geq 0,\ v > V_h,\ V_h > d_h + t \quad (15)$$

With increasing t, the marginal curtailment increases at a lower rate, implying that the marginal usable output decreases at a lower rate. As a result the cut-off point between the *high-* and *low-availability deployment range* ($v^{H|L} = V_h[\mu_h - \frac{\partial K_h^t}{\partial V_h} - \mu_l = 0]$) is reached for higher levels of V_h. As both parts of the *high-availability deployment range* are widened, the range is widened as a whole.

With increasing the transmission capacity, the *low-availability deployment range* is narrowed. This is because the width of the range is defined by $V_l = d_l - t$. For $t \geq d_l$, the *low-availability deployment range* disappears because output produced at node h can serve the entire demand at l. As a result, curtailments at node l already occur for initial capacities. Hence, there is no VRE penetration level when producers are incentivised to allocate additional VRE units solely to node l.

In the *split capacity deployment range*, producers increasingly allocate capacity to the high-availability node when transmission capacity increases. This is because, with increasing t, network restrictions get less relevant, such that producers can increasingly exploit the more favourable VRE conditions at node h.

End of Explanation.

Figure 3 demonstrates the insights from Finding NP 3 numerically. The numerical example displays the marginal allocation share at node h and the marginal usable outputs. Assumptions regarding the nodal demand (d_i), the availabilities ($B(\alpha_i, \beta_i)$) and the correlation among the availabilities ($\rho_{h,l}$) are identical to Figure 2.

First, marginal usable output is constant for $V_h \leq d_h + t$, such that the first part of the *high-availability deployment range* gets wider with increasing t. Second, the increase in marginal curtailment (i.e., the reduction in marginal usable output) is dampened with increasing t. Hence, the second part of *high-availability deployment range* gets wider. While for $t = \frac{1}{4}d_i$ the width the range is roughly $1.1d_i$, it is 50% wider for $t = \frac{3}{4}d_i$.

When transmission capacity exceeds the nodal demand ($t \geq d_i$), only differences in production patterns (arising when $\rho_{h,l} < 1$) incentivise the allocation of capacity to node l. For the given numerical example, this is relevant only when the $v > 5d_{h+l}$.

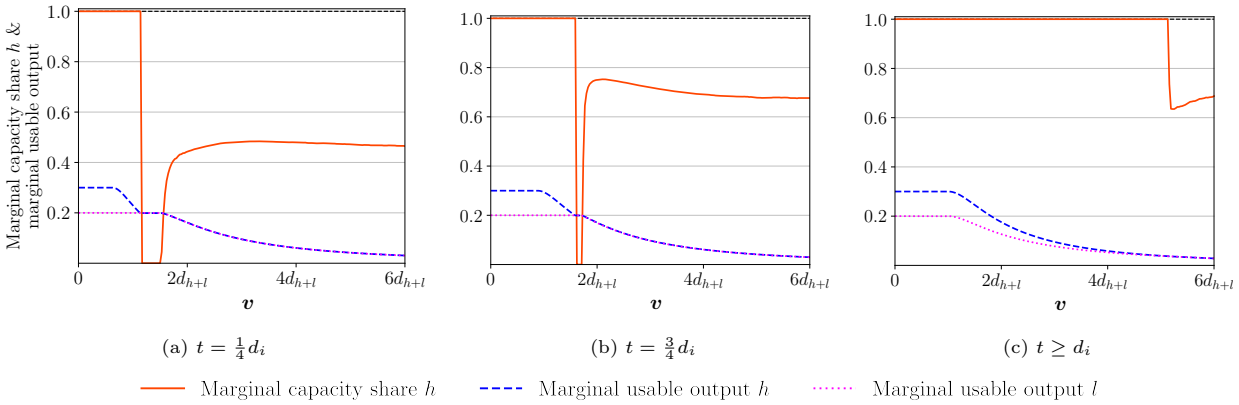

Figure 3: Effect of changes in the transmission capacity (t) on the spatial allocation ranges under nodal pricing.

Figure 3 also shows the shorting of the *low-availability deployment range*. While for $t = \frac{1}{4}d_i$ the range has a width of $\frac{4}{5}d_l$, the *low-availability deployment range* is narrowed to $\frac{1}{4}d_l$ if $t = \frac{3}{4}d_l$, and disappears if $t \geq d_l$. Lastly, the figure shows the shift towards the high-availability node in the *split capacity deployment range*. While for $t = \frac{1}{4}d_i$ roughly 50% of marginal capacity is placed to node h when $v = 4d_{h+l}$, the nodal marginal capacity share at node h increases to 70% for $t = \frac{3}{4}d_i$.

3.4. Effect of changes in the demand distribution

In this subsection, I derive the effect of the demand distribution on the capacity allocation ranges. Based on the analysis, I conclude:

Finding NP 4. *Under nodal pricing, increasing the demand at the high-availability node d_h widens the high-availability deployment range, while increasing d_l widens the low-availability deployment range. In the split capacity deployment range, the nodal share increases with the nodal demand.*

Explanation. Increasing the demand at node h widens the *high-availability deployment range*. This implies producers are willing to allocate capacity solely to the high-availability node for higher VRE penetration levels. This has two reasons: First, with increasing d_h, curtailment is absent for higher levels of V_h, as curtailment occurs when $V_h > d_h + t$. Second, the marginal curtailment arising from limited transmission capacity decreases with increasing d_h. These intuitive results can be shown mathematically by taking the derivative of Equation 11 with respect to d_h:

$$\frac{\partial^2 K_h^t}{\partial V_h \partial d_i} = -\frac{(\frac{d_i+t}{V_h})^{\alpha_h}(1-\frac{d_i+t}{V_h})^{-1+\beta_h}}{V_h B(\alpha_h,\beta_h)} < 0 \quad \text{for: } \alpha_h > 0,\ \beta_h > 0,\quad d_h > t \geq 0,\ v > V_h,\ V_h > d_h + t \quad (16)$$

As the result is negative in permissible domain, the marginal curtailment decreases in d_h, such that producers allocate capacity solely to node h for higher VRE penetration levels.

With increasing d_l the *low-availability deployment range* is widened. This is because the width of the range is defined by $V_l > d_l - t$.

In the *split capacity deployment range*, increases in nodal demand motivate producers to increase the share of capacity they allocate to the node. This is because the more nodal demand and nodal supply are aligned, the lower the need for transmission and resulting curtailments from limited transmission capacity. Hence, when the demand increases at one node, curtailments can be reduced by shifting capacity to that node. The reduction in curtailment implies increased usable output from VRE and decreased need for costly conventional power.

End of Explanation.

Figure 4 demonstrates the insights from Finding NP 4 numerically. Assumptions regarding the transmission capacity and the availability profiles are identical to Figure 2. When demand is mainly allocated to node l (i.e., $d_h = 25$ & $d_l = 75$), the *high-availability deployment range* is 5% smaller than the *low-availability deployment range*. Shifting demand from node l to node h widens the *high-availability deployment range* and narrows the *low-availability deployment range*. When demand is mainly allocated at node h (i.e., $d_h = 75$ & $d_l = 25$), the *high-availability deployment range* is 12 times as long as the *low-availability deployment range*. In the *split capacity deployment range*, the capacity share at node h increases from roughly 25% to 75% when shifting 50% of global demand from node l to node h.

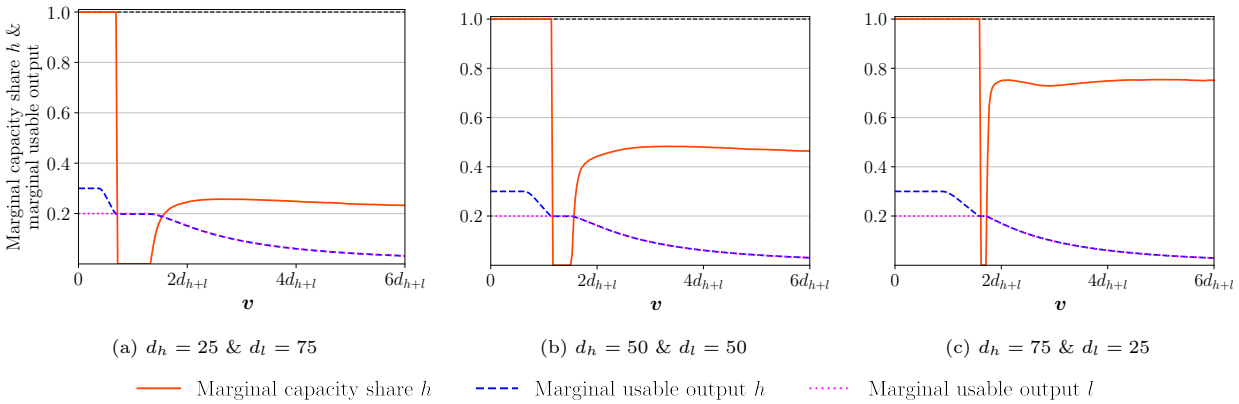

Figure 4: Effect of changes in the demand distribution on the spatial allocation ranges under nodal pricing.

3.5. Effect of changes in the availability profiles

In this range, I derive the effects arising from different features of the availability profiles on the capacity allocation ranges under nodal pricing. To do so, I analyse the effects of changes in the correlation among nodal availability profiles and changes in the average and the variance of nodal availability profiles.

3.5.1. Correlation

In this subsection, I derive the effect of the correlation among availability profiles on the capacity allocation ranges. Based on the analysis, I conclude:

Finding NP 5. *Under nodal pricing, changing the correlation among availability profiles $\rho_{h,l}$ does not affect the width of the high and low-availability deployment range. In the split capacity deployment range, increasing $\rho_{h,l}$ increases the capacity share allocated to the high-availability node. The effect increases with increasing t.*

Explanation. Under nodal pricing, changing the correlation among availability profiles $\rho_{h,l}$ does not affect the width of the *high-availability deployment range* because $\rho_{h,l}$ does not affect the nodal curtailment at node h when capacity at node l is absent. Changing the correlation does also not affect the width of the *low-availability deployment range*. This is because the width of the range is defined by $d_l - t$ for $\rho_{h,l} > -1$ as shown in the explanation of Finding NP 2. The correlation between availabilities does not affect the producers' allocation decision as long as VRE penetration is sufficiently low, so curtailment at node l is absent.

In the *split capacity deployment range*, increasing correlation shifts capacity towards the *high-availability node*. This is because the incentive for producers to allocate capacity to node l, namely exploiting the differences in availability profiles, is weakened with increasing correlation.

The extent of the effect increases with increasing transmission capacity (t). This is because, for low levels of t, the optimal allocation is mainly driven by the network restrictions. Producers reduce curtailment arising from limited transmission capacity to an appropriate level by allocating capacity relatively even among the nodes (see Finding NP 3). In such a case, the effect of correlation on the allocation is limited. Network restrictions are less relevant for high levels of t, and the availability profiles, including the differences in availability profile patterns, mainly drive the optimal allocation. Hence, the relevance of correlation on the producer's allocation decision in the *split capacity deployment range* increases with increasing t.

End of Explanation.

Figure 5 demonstrates the insights from Finding NP 5 numerically. Assumptions regarding the demand and the availability profiles are identical to Figure 2. The correlation varies in the interval 0 and 1 (i.e.,

$\rho_{h,l} \in [0,1]$) for the case of low and high transmission capacity (i.e., $t = \frac{1}{4}d_i$ and $t = \frac{3}{4}d_i$).

Independent of the transmission capacity, the width of the *high* and *low-availability deployment range* are not affected by changes in the correlation.

In the *split capacity deployment range*, increasing $\rho_{h,l}$ increases the capacity share of the high-availability node. Analysing the nodal marginal capacity shares at $v = 6d_{h+l}$ shows that the effect of correlation on node-h-capacity-share increases with increasing transmission capacity. For low levels of transmission capacity (i.e., $t = \frac{1}{4}d_i$), the node-h-capacity-share increases by only 10% from 43% to 53% when $\rho_{h,l}$ is increased from 0 (uncorrelated) to 1 (perfectly correlated). When transmission capacity is high (i.e., $t = \frac{3}{4}d_i$), the node-h-capacity-share increases by almost 30% (i.e., from 55% to 83%) when $\rho_{h,l}$ is increased from 0 to 1.

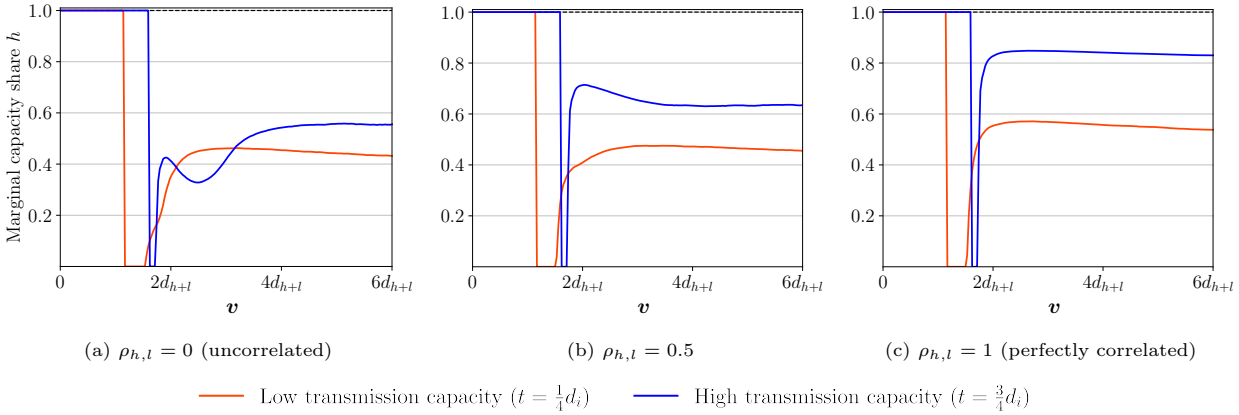

(a) $\rho_{h,l} = 0$ (uncorrelated) (b) $\rho_{h,l} = 0.5$ (c) $\rho_{h,l} = 1$ (perfectly correlated)

Figure 5: Effect of the correlation among availability profiles on the spatial allocation ranges under nodal pricing.

3.5.2. Average

In this subsection, I derive the effect of the average availability on the capacity allocation ranges. The density of availabilities is described by the parameters α_i and β_i. As stated in Section 2, increasing α_i primarily increases the average availability, while the variance remains rather constant. To assess the effect of changes in the average availability, I analyse the effects arising from changes in α_i.[6] Based on the analysis, I conclude:

Finding NP 6. *Under nodal pricing, increasing the average availability μ_l by increasing α_l narrows the high-availability deployment range. The effect of μ_h on the high-availability deployment range and the effect of μ_i on the split capacity deployment range is ambiguous and depends on the system topology.*

Explanation. With increasing average availability at node l the *high-availability deployment range* is narrowed,

[6] Changing μ_i while keeping the variance fully constant, i.e. also altering β_i, does not alter the findings. However, such an approach does not allow for analysing the effects analytically.

because the marginal potential output at node l increases with increasing μ_l:

$$\frac{\partial^2 PO_i}{\partial V_i \partial \alpha_i} = \frac{\partial \mu_i}{\partial \alpha_i} = \frac{\beta_i}{(\alpha_i + \beta_i)^2} > 0 \quad \text{for: } \alpha_i > 0,\ \beta_i > 0 \tag{17}$$

As a result, producers only tolerate lower marginal curtailment levels at node h when allocating capacity to the node. This implies a narrowing of the *high-availability deployment range*.

Increasing the average availability at node h either narrows or widens the *high-availability deployment range*. This is due to two opposing effects: On the one hand, increases in the nodal availability increase the marginal potential output as shown in Equation 17. This effect incentives producers to widen the sole capacity allocation to node h. On the other hand, increases in nodal availability increase the marginal curtailment arising from limited transmission capacity. The increased relevance of network restrictions and the resulting increase in marginal curtailments incentive producers to narrow the sole capacity allocation to node h. Subtracting both effects yields the effect on the marginal usable output. This is given by the following expression:

$$\frac{\partial^2 UO_i}{\partial V_i \partial \alpha_i} = \frac{B_{\frac{d_i+t}{V_i}}(\alpha_i+1,\beta_i)\left(\log\left(\frac{d_i+t}{V_i}\right)+\psi^{(0)}(\alpha_i+\beta_i)-\psi^{(0)}(\alpha_i)\right)}{B(\alpha_i,\beta_i)} - \frac{\left(\frac{d+t}{V_i}\right)^{\alpha_i}{}_3F_2\left(\alpha_i+1,\alpha_i+1,1-\beta_i;\alpha_i+2,\alpha_i+2;\frac{d+t}{V_i}\right)}{\frac{V_i(1+\alpha_i)^2}{d+t}B(\alpha_i,\beta_i)} \tag{18}$$

Depending on the parameters t, d_i, and $\beta_i(\alpha_i, \beta_i)$ as well as the nodal VRE capacity, V_i, the expression is positive or negative. When t is low, the term tends to be negative in the relevant domain. Hence, when network restrictions are tight, the increase in marginal curtailment due to limited transmission capacity outweighs the increase in marginal potential output. In such a situation, producers reduce the amount of capacity they solely allocate to node h, with increasing μ_h. When t is high, the term tends to be positive in the relevant domain. Hence, with increasing μ_h, producers increase the capacity they solely allocate to node h.

The width of the *low-availability deployment range* is given by $d_l - t$, such that it is not affected by μ_i.

The effect of increasing average availability on the *split capacity deployment range* is ambiguous. This is also due to the two opposing effects of increased potential output and curtailments. While producers tend to increase the nodal with increasing μ_i when t is high, the opposite is true for low levels of t.

End of Explanation.

Figure 6 displays the effects of changes in the average nodal availability on the capacity allocation in a

numerical example. Assumptions regarding the demand, q_i, and the correlation are identical to Figure 2. To analyse the effect for low and high levels of transmission capacity, the marginal capacity shares are calculated for $t = \frac{1}{10}d_i = 5$ and $t = \frac{3}{4}d_i = 37.5$.

When increasing μ_l from 0.2 to 0.25, the *high-availability deployment range* narrows by roughly 17% for both cases of transmission capacity (compare Figure 6a and c). All other effects when changing μ_i highly depend on the level of transmission capacity. In the numerical example, this can be observed best for the *split capacity deployment range*. When transmission capacity is low, a higher μ_h decreases the share of capacity allocated to node h by roughly 10-15 percentage points and increasing μ_l decreases the share of capacity allocated to node l by roughly 10-20 percentage points. When transmission capacity is high, the opposite effects occur. Higher μ_h increases the share of capacity allocated to node h by roughly five percentage points. Higher μ_l decreases the share of capacity allocated to node l by roughly 10-20 percentage points.

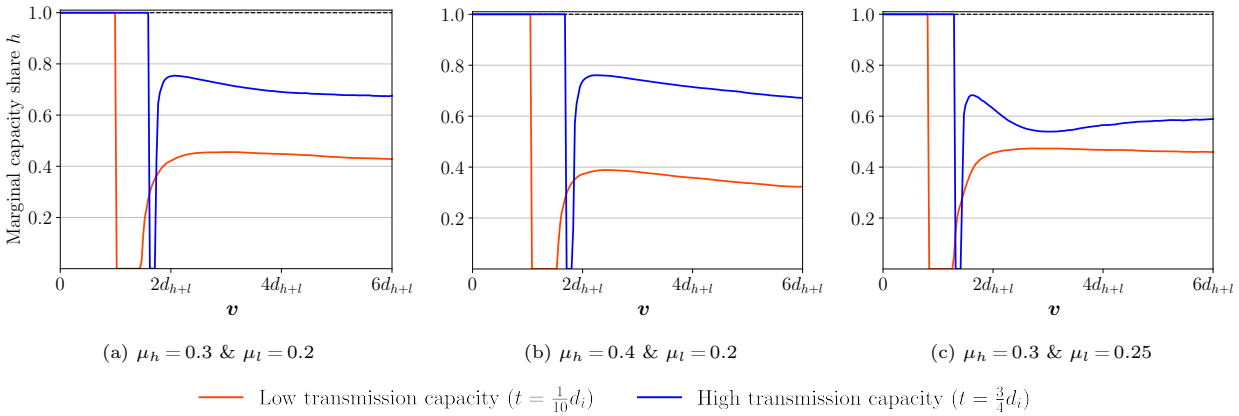

Figure 6: Effect of the average in the availability profile on the spatial allocation ranges under nodal pricing.

3.5.3. Variance

In this subsection, I derive the effect of the variance in availability profiles (σ_i^2) on the capacity allocation ranges. The variance is defined by the availabilities density function, i.e., $B(\alpha_i, \beta_i)$. To analyse the effect of σ_i^2, the parameter values α_i and β_i are changed such that the average output potential μ_i remains constant. Based on the analysis, I conclude:

Finding NP 7. *Under nodal pricing, higher variance at the high-availability node σ_h^2 narrows the high-availability deployment range. The effect of increases in the nodal variance on the split capacity deployment range is twofold: The nodal share decreases for moderate VRE penetration or high transmission capacity, while the nodal share increases when VRE penetration is high, and transmission capacity is low.*

Explanation. Under nodal pricing higher σ_h^2 narrows the *high-availability deployment range*. This is because

the volatile potential output decreasingly matches constant demand. As a result situations, in which the potential output exceeds $d_h + t$ and curtailments are present, occur more often. When marginal curtailments are higher the usable output at node h is equal to the potential output at node l for lower levels of V_h.
The width of the *low-availability deployment range* is given by $d_l - t$, such that it is not affected by σ_i^2. The effect of increases in variance on the *split capacity deployment range* is twofold. On the one hand, increases in the variance reduce the overall usable output as the potential output decreasingly matches the nodal demand. As a result, increasing the variance reduces the marginal usable output for low and moderate levels of VRE penetration. Producers are incentivised to allocate less VRE to the node with increased variance. On the other hand, increasing the nodal variance can increase the marginal usable output for high levels of VRE penetration. This is because increases in the nodal variance lower the nodal VRE share. When nodal VRE shares are high (e.g. close to 100%), additional VRE can be barely used to serve the nodal demand. With lower VRE shares, due to increases in the variance, a higher share of the additional VRE can be used to serve the nodal demand and thereby increase the marginal usable output. Hence, producers are incentivised to allocate more VRE to the node with increased variance when VRE penetration is high. The higher the VRE penetration, the stronger the effect. The effect gets weaker with increasing transmission capacity because VRE output can be increasingly integrated by exports and high nodal VRE shares get less relevant.

End of Explanation.

Figure 7 displays the insights from Finding NP 7 numerically for the case of low transmission capacity (i.e., $t = \frac{1}{10} d_i$).[7] Assumptions regarding the demand, the average availability, and the correlation are identical to Figure 2. When the variance is increased at node h (compare Figure 7a and b), the *high-availability deployment range* is narrowed from $1.3d_{h+l}$ to $0.9d_{h+l}$. Additionally, the figure confirms that the effect on the *split capacity deployment range* is twofold. In the case of moderate VRE penetration levels (i.e., roughly $v \leq 4d_{h+l}$), increasing σ_h^2 lowers the share of capacity allocated to node h . Such changes occur for VRE shares below 70%, as indicated by the green line. For high VRE penetration levels (i.e., $v \leq 4d_{h+l}$ or a VRE share above 70%), increasing σ_h^2 increases the share of capacity allocated to node h. Comparing the green lines also illustrates the decrease in the global VRE share. When the variance is increased at node l (compare Figure 7a and c)), the *high-availability deployment range* is not affected. The effect on the *split capacity deployment range* is the same as in the case of increases in σ_h^2. For moderate VRE penetration levels, higher σ_l^2 lower the share of capacity allocated to node l (i.e., more capacity is allocated to node h). For high VRE

[7] A numerical analysis for the case of high transmission capacity is shown in Appendix D.

penetration levels, higher σ_l^2 increase the share of capacity allocated to node l.

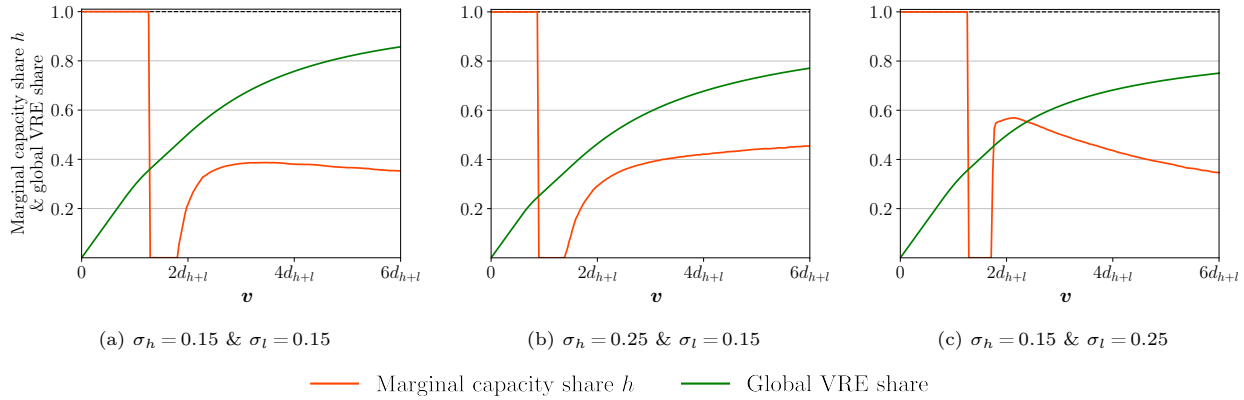

(a) $\sigma_h = 0.15$ & $\sigma_l = 0.15$ (b) $\sigma_h = 0.25$ & $\sigma_l = 0.15$ (c) $\sigma_h = 0.15$ & $\sigma_l = 0.25$

Figure 7: Effect of the variance in the availability profile on the spatial allocation ranges under nodal pricing.

4. Spatial allocation under uniform pricing

In this section I analyse the socially optimal spatial allocation under uniform pricing. The structure is similar to the previous section. First, I derive the spatial allocation rationale of producers facing uniform pricing. Then, the ranges in which capacity allocation can be grouped are identified. Within the analysis I assess the inefficiency by comparing the results to the optimal spatial allocation I derived in section 3. In a last step, it is analysed how various parameters of the system topology, namely the transmission capacity, the demand distribution, and the characteristics of the VRE availability profile, drive the spatial allocation and the resulting inefficiencies. Thereby the interactions among the parameters is assessed.

4.1. Spatial allocation rationale

In this subsection, I derive the spatial allocation rationale in the presence of uniform pricing, perfect competition, and perfect foresight. I conclude that:

Finding UP 1. *Under uniform pricing, producers aim to allocate the capacity such that their marginal profits are identical at both nodes. If marginal profits differ independently of the capacity allocation, producers allocate all capacity to the node with a higher marginal profit.*

Explanation. Uniform pricing implicitly ignores network constraints when deriving market prices. Hence, the producers' profit maximisation problem coincides with minimising the total costs when ignoring network constraints, denoted by DTC. The DTC are given by the global output of the conventional technology before redispatch times the marginal costs of the conventional technology (c). The global output of the

conventional technology before redispatch arises from the global demand minus the global output of the VRE technology sold to the market. The global output of the VRE technology sold to the market is given by the potential output minus the output, which cannot be sold to the market. Output cannot be sold to the market when the sum of nodal VRE capacity times the nodal availability ($\sum_i V_i \, avail_i$) exceeds the global demand (d_{h+l}). The integral over time of all output which cannot be sold to the market I denote as zero profit potential (ZPP) and is described by the following formula :

$$ZPP = \int_0^1 \sum_i V_i \, AVAIL_i(\mu_i, \sigma_i^2)[\sum_i V_i \, avail_i > d_{h+l}] \tag{19}$$

The relationship between demand, zero profit potential, as well as the different types of output is illustrated in Figure 8.

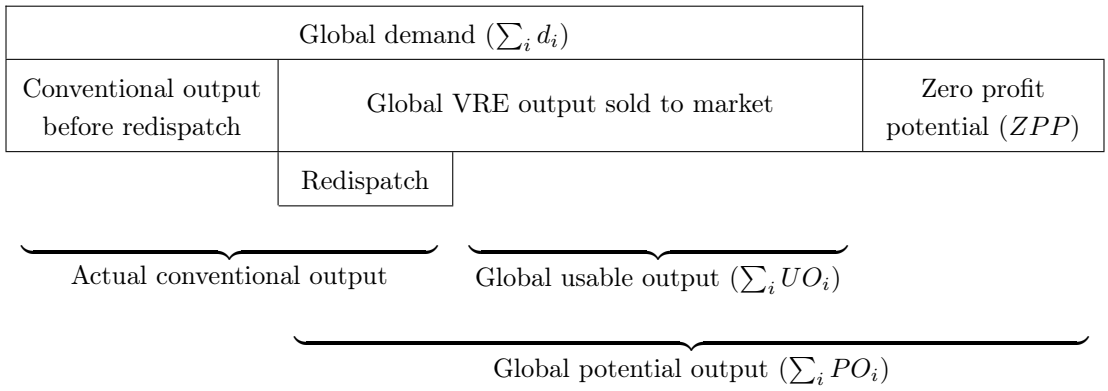

Figure 8: Relationship between demand, zero profit potential, as well as potential, saleable, and usable output under uniform pricing.

Based on the figure and explanation above the objective function for the case of uniform pricing can be derived:

$$\min_{V_h} \; DTC = \Big(\int_0^1 d_{h+l} - \big(\sum_i PO_i(V_h) + ZPP(V_h) \big) \Big) c \tag{20}$$

The cost minimisation problem is solved by equating the derivative of Equation 20 with respect to V_h. Restructuring and resubstituting $v - V_h$ with V_l yields to the following equilibrium:

$$\underbrace{\frac{\partial PO_h}{\partial V_h}}_{\substack{\text{marginal} \\ \text{potential in } h}} - \underbrace{\frac{\partial ZPP}{\partial V_h}}_{\substack{\text{marginal zero} \\ \text{profit potential}}} = \underbrace{\frac{\partial PO_l}{\partial V_l}}_{\substack{\text{marginal} \\ \text{potential in } l}} - \underbrace{\frac{\partial ZPP}{\partial V_l}}_{\substack{\text{marginal zero} \\ \text{profit potential}}} \tag{21}$$

The optimal V_h and V_l ensure that the difference between marginal potential output and marginal zero profit

potential is identical at both nodes. The marginal potential output only generates a profit when it can be sold to the market. In these cases the price is set by the marginal costs of the conventional technology, c. Therefore, the difference between the marginal potential output and the zero profit potential times c represent the marginal profit:

$$\frac{\partial \text{Profit}_i}{\partial V_i} = \left(\frac{\partial PO_i}{\partial V_i} - \frac{\partial ZPP_i}{\partial V_i}\right)c \tag{22}$$

Hence, producers maximise their profits by allocating the VRE capacity such that the marginal profit is identical at both nodes. If Equation 21 does not hold for any permissible spatial allocation (i.e., $V_h \in (0, v)$), producers maximise their profits by allocating all capacity to the node, offering higher marginal profits.

End of Explanation.

Plugging in the Beta distribution allows us to calculate the marginal potential output. As in the case of nodal pricing, it is given by $\frac{\partial PO_i}{\partial V_i} = \mu_i = \frac{\alpha_i}{\alpha_i+\beta_i}$. The zero profit potential depends on the joint distribution of the availabilities in h and l. The joint distributions depend on the specific beta distribution parameters α_i and β_i, the correlation $\rho_{h,l}$, and the demand d_i. The zero profit potential and their marginal cannot be derived analytically in a universal manner, such that the values are calculated numerically in following subsections.

4.2. Capacity allocation ranges

In this subsection, I derive the capacity allocation ranges which occur based on the spatial allocation rationale under uniform pricing. I conclude that:

Finding UP 2. *Under uniform pricing, the spatial VRE allocation encompasses the high-availability deployment range and the split capacity deployment range. Allocation is efficient when VRE penetration is low. With increasing VRE penetration inefficiencies emerge. These resulting welfare losses increase until capacity is split among nodes.*

Explanation. First, producers allocate capacity to the high-availability node (i.e., *high-availability deployment range*). Producers behave like that, because for $V_i < d_{h+l}$ the conventional technology ($p = c$) sets the price at both nodes independent of network restriction. When network restrictions prevent the transmission of some VRE output traded among the nodes these volumes are curtailed, but producers still receive the payment. The unsatisfied demand is served by conventional power plants, which are located to the appropriate node. The provision of these volumes induce costs of c per unit, which are paid by the consumers.

Hence, producers earn $\mu_i c$ with each unit of capacity for $V_i < d_{h+l}$. As $\mu_h > \mu_l$, producers maximise their profits by allocating the capacity solely to the node h. When V_h exceeds d_{h+l} the marginal profits at node h

and l decrease. The marginal profit decreases faster at h than at node l, when the availability profiles are not perfectly correlated $\rho_{h,l} < 1$. Because VRE production follows the availability profile of node h prices are zero when the availability in h is high and prices equal c, when availabilities are low. When nodal availability profile patterns differ, potential output at node l could be sold for higher average prices than at node h. When marginal profits are identical at both nodes, the *high-availability deployment range* ends.
To maximise profits, producers split additional capacity among the two nodes, such that the nodal marginal profits are identical.

Allocation is efficient, when the highest possible global usable output for a given VRE penetration is achieved. Such a global usable output is achieved under nodal pricing and can be denoted as $UO^{NP}_{h+l}(v)$. The global usable output achieved under uniform pricing can be denoted as $UO^{UP}_{h+l}(v)$. When the usable output is lower under uniform pricing, the welfare loss is given by the reduction in usable output compared to the optimum times the marginal costs for conventional technology:

$$\text{Welfare Loss}(v) = \big(UO^{NP}_{h+l}(v) - UO^{UP}_{h+l}(v)\big)c \tag{23}$$

As the global VRE share is given by dividing the usable output with the global demand, the following relationship between the welfare loss and the reduction in the global VRE share exists:

$$\text{Reduction in global VRE share}(v) = \frac{\text{Welfare Loss}(i)}{d_{h+l}c} \tag{24}$$

When VRE penetration is sufficiently low capacity is allocated to node h under uniform and nodal pricing, such that the UO_{h+l} is identical under both regimes and welfare losses are absent. Welfare losses occur in the *high-availability deployment range*, when the marginal usable output node l exceeds the marginal usable output at node h. This is because from that point onward it is inefficient to allocate marginal capacity solely to node h. In this case the global usable output is below maximum possible for the given v. Welfare loss grow as long as producers solely allocate capacity to node h.
When capacity is split among the two nodes (i.e., *split capacity deployment range*), welfare losses are partly mitigated. This is because capacity allocated to node l is not curtailed, such that the average marginal usable output of both nodes exceeds the marginal usable output under nodal pricing.

End of Explanation.

Figure 9 demonstrates the insights from Finding UP 2 numerically. The parameters are identical to Figure 2. By setting $c = \frac{1}{d_{h+l}}$, the welfare loss coincides with the reduction in the global VRE share.

The upper diagram shows that capacity is allocated solely to the high-availability node when $v < 5.1d_{h+l}$. Welfare losses arise for $v > v^{H|L}$, where $v^{H|L}$ defines the value separating the *high-* and *low-availability deployment range* under nodal pricing. For $v > v^{H|L}$ the marginal usable output of node h subceeds the one of node l, such that welfare would be increased when some VRE would be shifted to node l. The welfare losses grow with increasing VRE penetration. At $v = 5.1d_{h+l}$, welfare losses reach their maximum. Due to the inefficient allocation, less than 55% of demand can be served with VRE, compared to 75% under an optimal allocation. Hence, conventional power needs to serve an additional 20% of demand, inducing costs of $0.2d_{h+l}c = 0.2$. This is the case even though the potential output of VRE is 20% higher under uniform pricing than under nodal pricing. These numbers imply 65% of VRE is curtailed on average and 95% of marginal output is curtailed.

When $v > 5.1d_{h+l}$ capacity is split among the nodes h and l in a roughly 70/30 ratio. As no output is curtailed at node l, welfare losses compared to the social optimum slightly decline.

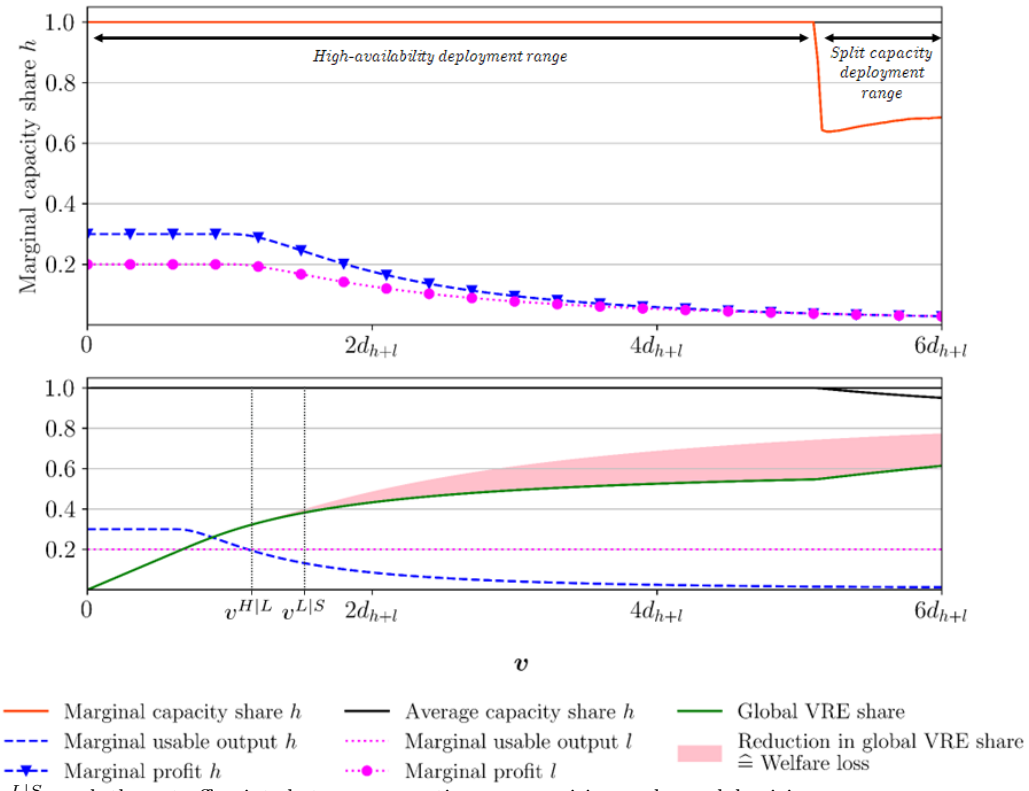

$v^{H|L}$ and $v^{L|S}$ mark the cut-off points between respective ranges arising under nodal pricing.

Figure 9: Spatial allocation, marginal usable output, marginal profits, VRE shares and welfare losses at different VRE penetration levels under uniform pricing.

4.3. Effects of changes in the transmission capacity and demand distribution

In this subsection, I derive the effect of changes in the transmission capacity t and the demand distribution on the capacity allocation and welfare. Based on the analysis, I conclude:

Finding UP 3. *Under uniform pricing, the transmission capacity and the demand distribution do not affect the capacity allocation. With increasing t, welfare losses decrease. Allocation is efficient when $t > d_i$. Distributing demand more according to potential output also reduces welfare losses.*

Explanation. The transmission capacity and the demand distribution do not affect the capacity allocation. This is because curtailment arising from network restrictions is ignored under uniform pricing.
As curtailment arising from network restrictions affect the socially optimum capacity allocation, the transmission capacity and the demand distribution affect the efficiency. The deployment under uniform pricing coincides with the one under nodal pricing, when transmission capacity allows to serve the demand at node l, even when capacity is allocated solely at node h, i.e., $t > d_i$. Hence, welfare losses are absent when $t \geq d_i$. With decreasing t, welfare losses increase. This is because with decreasing t, it is optimal to allocate more capacity to node l to reduce curtailments.
Distributing nodal demand more according to potential output reduces the need for transmission. Hence, distributing demand more according to potential output also reduces the level of curtailments arising from network restrictions and welfare losses.

End of Explanation.

Figure 10 displays the effect of changes in the transmission capacity and the demand distribution.[8]
Independent of the transmission capacity and the demand distribution, capacity is allocated to node h until $v = 5.1 d_{h+l}$. For the same VRE penetration level, welfare losses are highest. The welfare loss decreases with increasing t. For low transmission capacity, i.e., $t = \frac{1}{4} d_{h+l}$, welfare losses equivalent to the variable costs, when serving 20% of global demand with conventional power, occur. The welfare loss is more than halved when transmission capacity is tripped, and welfare losses disappear for $t > d_i$. Furthermore, the higher t, the later welfare losses emerge.
With demand increasingly located at node h, the welfare losses decreases. When 75% of demand is located at node h, welfare losses are only one-fifth compared to the case when 75% of demand is located at node l.

[8] The parameters in Figure 10a are identical to Figure 3, while the parameters in Figure 10b are identical to Figure 4. By setting $c = \frac{1}{d_{h+l}}$, the welfare loss coincides with the reduction in VRE share.

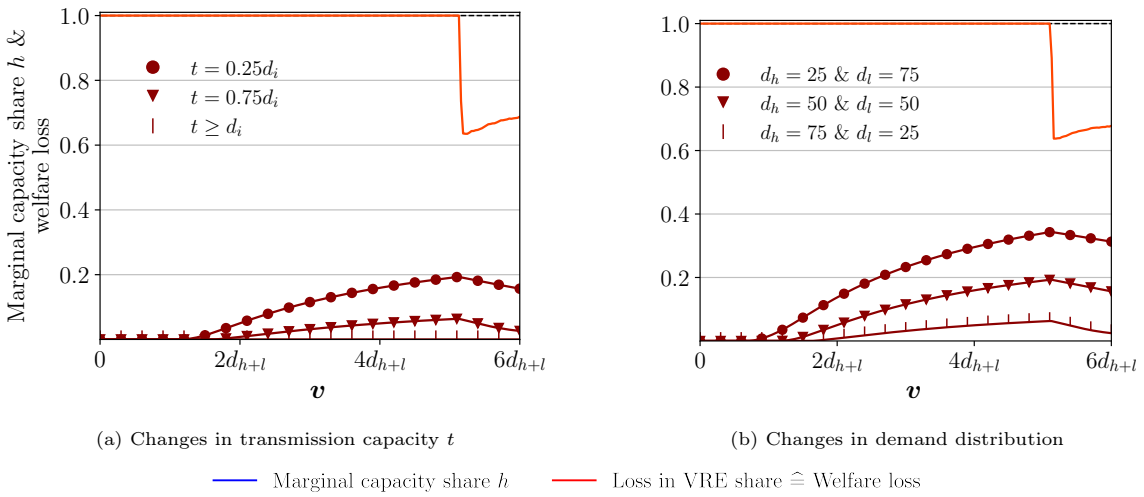

(a) Changes in transmission capacity t

(b) Changes in demand distribution

Figure 10: Effects of changes in the transmission capacity and demand distribution on the spatial allocation ranges and welfare losses under uniform pricing.

4.4. Effect of changes in the availability profiles

In this section, I derive the effects arising from different features of the availability profiles on the ranges of the capacity allocation under uniform pricing. To do so, I analyse the effects of changes in the correlation among nodal availability profiles and changes in the average and the variance of nodal availability profiles. Based on the analysis, I conclude:

Finding UP 4. *Under uniform pricing, the availability profiles affect the spatial allocation. The effect on the high-availability deployment range and the split capacity deployment range is identical to the case of nodal pricing and $t \geq d_i$. For $t < d_i$, the effect on the spatial allocation are stronger under uniform pricing. Changes in the availability profiles, which incentivise capacity to be allocated more according to demand, reduce welfare losses.*

Explanation. The availability profiles affect the spatial allocation because the global supply is affected. The effect on the spatial allocation of VRE is stronger than under nodal pricing if transmission capacity is binding. This is because, under nodal pricing the effects on the capacity allocation arising from availability profiles are mitigated by curtailments arising from limited transmission capacity. The higher t, the lower the mitigation and the higher the impact of availability profiles. For $t \geq d_i$, the availability profiles affect the allocation in the same way under uniform and nodal pricing.

Changes in the availability profiles also affect the level of inefficiency. If changes in the availability profiles incentivise a capacity allocation which induces potential output to be allocated more according to demand, welfare losses are reduced. This is because, with the increasing alignment of potential nodal output and

nodal demand, less potential output needs to be transmitted, and less output is curtailed due to limited transmission capacity. Thereby the redispatch-level of conventional power plants decreases, reducing costs and increasing welfare and the global VRE share. Depending on the demand distribution, the availability profiles, which minimise the welfare loss differ. *End of Explanation.*

4.4.1. Correlation

When availabilities are perfectly correlated, producers allocate capacity solely to the high-availability node (i.e., node h). The lower the correlation, the more often the availability at node l exceeds the availability at node h. Producers exploit these differences in the availability profile by allocating some capacity to node l. Hence, with decreasing correlation, producers allocate more capacity to node l. The effect on welfare depends on the demand distribution. When demand $d_l \geq d_h$, decreasing the correlation decreases the need for transmission and curtailments arising from limited transmission capacity. Hence, low $\rho_{h,l}$ lead to low welfare losses compared to the social optimum. However, when demand is located mainly at node h, the need for transmission is lowest, and resulting curtailments are lowest when the correlation is high. Hence, high $\rho_{h,l}$ lead to low welfare losses compared to the social optimum.

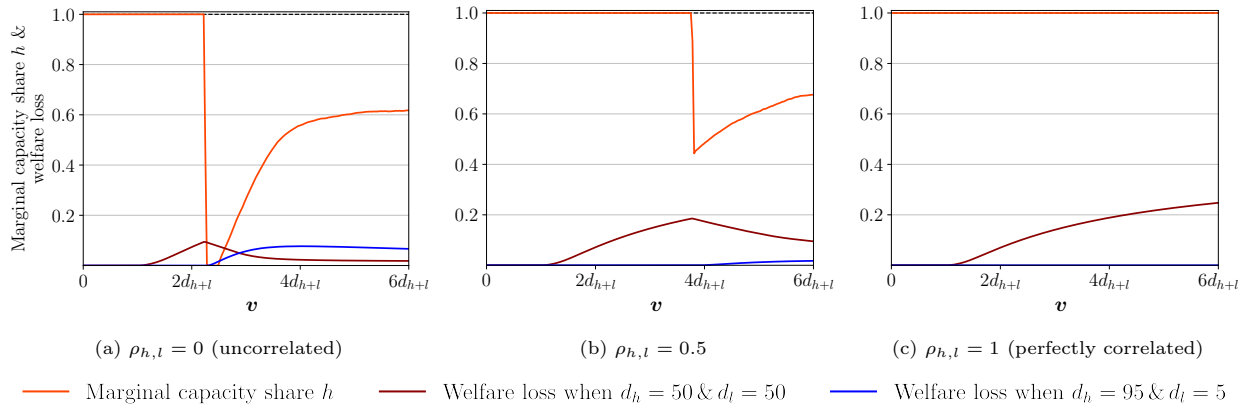

Figure 11: Effect of the correlation among availability profiles on the spatial allocation ranges and welfare losses under uniform pricing.

Figure 11 illustrates these results.[9] Capacity is solely allocated to node h for all levels of analysed VRE penetration when availability profiles are perfectly correlated. In contrast, when availability profiles are uncorrelated, 38% to 100% of marginal VRE capacity is allocated to node l for $v > 2.5d_{h,l}$. Which level of correlation yields the lowest welfare loss depends on the demand distribution. When demand is equally distributed, welfare losses are lowest when availability profiles are uncorrelated. In contrast, when 95% of

[9]The average and the variance of the availability profiles are identical to Figure 9. To better identify the effect on welfare losses, $t = 5$ is assumed. By setting $c = \frac{1}{d_{h+l}}$, the welfare loss coincides with the reduction in the VRE share.

demand is concentrated at node h, welfare loss remains absent in the analysed VRE penetration domain when the correlation is perfect.

4.4.2. Average

Under uniform pricing, a higher average nodal availability incentivises producers to allocate more VRE capacity to the respective node. This is because producers only consider the increase in the potential nodal output. The increasing curtailments arising from limited transmission capacity are ignored. As $\mu_h > \mu_l$, producers allocate more capacity to node h. With an increasing difference in availabilities the share of capacity allocated to node h increases.

Hence, when demand $d_l \geq d_h$, decreasing the differences in availability decreases the need for transmission and hence decreases the welfare loss. However, when demand is concentrated at node h, the need for transmission and the resulting welfare losses from curtailment is lowest when differences in availability are substantial.

Figure 12 illustrates these results.[10] Capacity is solely allocated to node h for all levels of analysed VRE penetration when the average availability at node h is 2.3 times as high than at node l (i.e., $\mu_h = 0.35$ and $\mu_l = 0.15$). In contrast, 40-100% of marginal VRE capacity is allocated to node l for $v > 1.9 d_{h,l}$, when the average availability at node h is only 17% higher than at node l (i.e., $\mu_h = 0.27$ and $\mu_l = 0.23$).

Which level of correlation yields the lowest welfare loss depends on the demand distribution. When demand is equally distributed, welfare losses are lowest when average availabilities barely differ. In contrast, when 95% of demand is concentrated at node h, welfare losses remain absent in the analysed VRE penetration domain when availabilities are 2.3 times higher at node h than at node l.

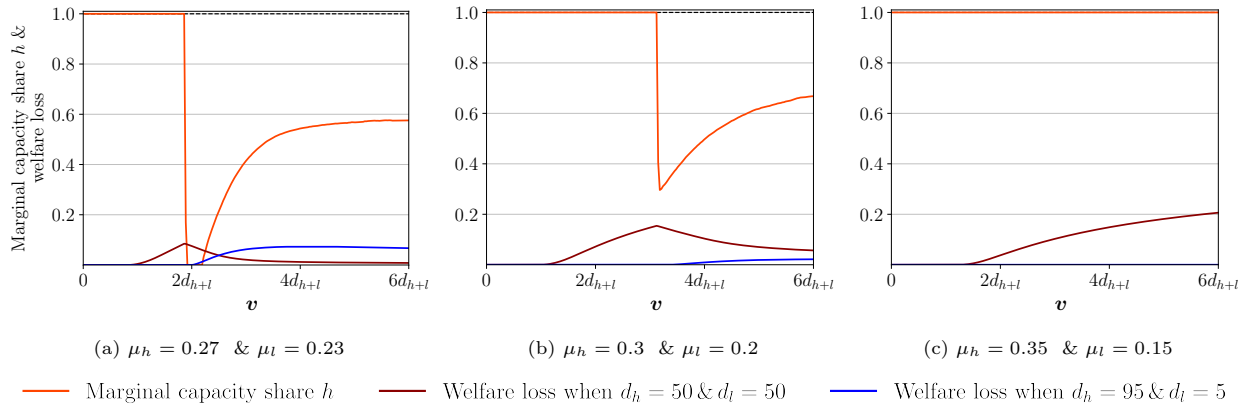

Figure 12: Effect of the average availability on the spatial allocation ranges and welfare losses under uniform pricing.

[10] The variance of the availability profiles varies between X and Y, which is very close to the variance assumed in Figure 10. To better identify the effect on welfare losses, a low transmission capacity of $t = \frac{d_{h+l}}{10}$ and a moderate correlation of $\rho_{h,l} = 0.4$ is assumed. By setting $c = \frac{1}{d_{h+l}}$, the welfare loss coincides with the reduction in VRE share.

4.4.3. Variance

Under uniform pricing, a higher nodal variance incentivises producers to allocate less VRE capacity to the respective node. This is because, with increasing nodal variance, the nodal output more likely exceeds the global demand. In such situations, prices are zero, and some potential output cannot be sold. To reduce the share of such situations, producers allocate less VRE to the node with increased variance.

Hence, when demand $d_l \geq d_h$, increasing the variance at node h or decreasing the variance at node l decreases the need for transmission and curtailments arising from limited transmission capacity. Such changes in the variance also decrease the welfare loss compared to the social optimum. When demand is concentrated at node h, the need for transmission and the resulting welfare losses from curtailment is lowest when the variance at node h is low compared to the variance at node l.

These results are illustrated in Figure 12.[11] Capacity is solely allocated to node h for all levels of analysed VRE penetration when availability profiles at both nodes share the same variance (i.e., $\sigma_h = \sigma_l = 0.2$). In contrast, 65-100% of marginal VRE capacity is allocated to node l for $v > 3d_{h,l}$, when the variance at node h is 50% higher than at node l (i.e., $\sigma_h = 0.24$ and $\sigma_l = 0.16$).

Which level of correlation yields the lowest welfare loss depends on the demand distribution. When demand is equally distributed, welfare losses are lowest when the variance is 50% higher at node h. In contrast, when 95% of demand is concentrated at node h, welfare losses remain absent in the analysed VRE penetration domain when the variance is identical at both nodes.

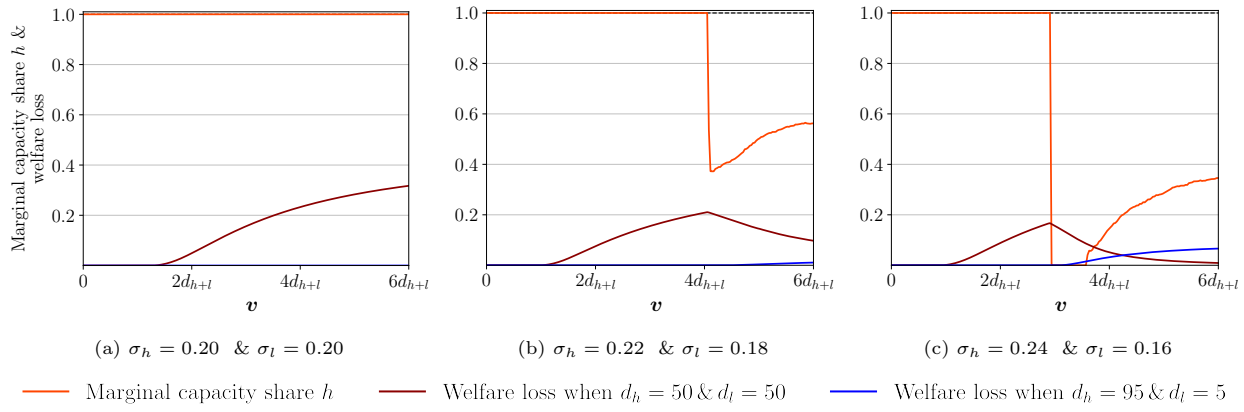

Figure 13: Effect of the average availability on the spatial allocation ranges and welfare losses under uniform pricing.

[11]The assumed average in the availability profiles is identical to Figure 7, and the assumed transmission capacity, correlation, as well as variable costs of the conventional technology, are identical to Figure 12.

5. Discussion

The paper shows that optimal VRE allocation can be grouped into three ranges. At low levels of VRE penetration, capacity should be allocated to the node with higher average availability (i.e. *high-availability deployment*). When curtailments fully remove the advantage in usable output of the high-availability node, additional capacity should be allocated to the node with lower availability (i.e., *low-availability deployment range*). When curtailment is present at both nodes, the capacity should be split (i.e., *split capacity deployment range*). Policymakers designing instruments to expand the VRE capacity should consider the range they are in. Countries starting to deploy in VRE should incentivise the placement of initial capacities in regions with high availability. Countries that already have significant VRE capacity in regions with a high average availability may be better off when incentivising (some) investment in regions with lower availability.

The width of the *high* and the *low-availability deployment range*, as well as the nodal capacities shares in the *split capacity deployment range*, are found to depend on the transmission capacity, the demand distribution, and the availability profiles. These characteristics vary among countries. In the UK, compared to Germany, the average wind availability is higher, the regional difference is lower, and the correlation among the availability profiles is lower (Staffell and Pfenninger, 2016; Sinden, 2007). As a result, the *high* and *low-availability deployment range* are narrower in the UK than in Germany due to lower differences in availability and higher average availabilities when assuming similar transmission capacity and demand distribution.

Under uniform pricing, the dominant market design, producers are found to allocate capacity to the high-availability node for higher VRE penetration levels than socially optimal. This is because curtailments arising from limited transmission capacity, which would encourage producers to allocate capacity more according to demand, are ignored. Welfare losses occur when curtailments from limited transmission capacity fully diminish the advantage in usable output of the high-availability node. The welfare losses increase until differences in availability profiles incentivise allocating some capacity to the low-availability node.

Hence, countries with uniform pricing that start to deploy VRE or feature low VRE shares do not have to implement additional measures to improve the spatial allocation. In line with the findings of this paper, in Japan, VRE only serves 6% of demand, and support schemes do not differentiate spatially (IEA, 2022a). Countries with uniform pricing, which already deploy substantial VRE capacity, such as Germany, should consider measures encouraging producers to invest in areas with lower availabilities.

The welfare losses under uniform pricing decreases in the level of transmission capacity and increases in the need for transmission. The latter is found to be influenced by the demand distribution and the availability

profiles. Welfare losses are, for instance, small when transmission capacity is high compared to nodal demand or demand is allocated mainly to the high-availability node. In contrast, welfare losses are found to be high when transmission capacity is low, demand is concentrated in the low-availability node and availability profiles incentive an allocation to the high-availability node (e.g., high difference in nodal availabilities). Such circumstances are, for example, present in Germany. This is in line with the finding from ACER (2022), who show that splitting Germany into two market zones would yield larger welfare increases than splitting market zones in other EU countries.[12] Hence, policymakers should take into account the given transmission capacities, the demand distribution, and regional availability profiles when considering to split their market zone or to implement spatially differentiated VRE subsidies.

The findings of my analysis confirm and extent the findings of the papers presented in Section 1. The results of Kies et al. (2016) suggest that with an increasing VRE penetration, it is optimal to increasingly allocate capacity to regions with a low average availability. My findings extend the result by showing that the optimal spatial allocation of VRE can be grouped into three ranges.

Pechan (2017) finds that under nodal pricing, producers increasingly concentrate capacity at high-availability nodes when the correlation increases and when the variance in high-availability nodes is low. This is in line with my analysis. My research adds the finding that the effect of correlation becomes more relevant with increasing transmission capacity.

In the case of uniform pricing, Pechan (2017) does finds no effect of correlation and variance on the allocation under uniform pricing. This is because she only analyses a case with a moderate VRE share. I can show that the capacity allocation is affected once the VRE penetration reaches a certain threshold.

In line with my analysis, a welfare loss arises in Schmidt and Zinke (2020) due to an inefficient allocation of VRE. The identified welfare loss of 1.5% seems low compared to numerical results in my analysis. This is because, in my analysis, a case with similar correlation, similar demand distribution and similar VRE penetration leads to a welfare loss of roughly 15%. [13] The difference in welfare loss mainly arises due to the following two aspects: First, Schmidt and Zinke (2020) only assess the allocation of wind onshore capacities added in the years 2020 to 2030. These capacities produce less than 20% of the VRE output. The remaining 80% come from onshore wind built before the year 2020, offshore wind and solar power. These capacities are distributed identically under uniform and nodal pricing in their analysis. Second, Schmidt and Zinke

[12] Splitting a country into two market zones allows prices to differ when transmission capacities between the new market zones are congested. Such a market design is an intermediate design of uniform pricing and nodal pricing.

[13] In Figure 10b the case with a 25% demand allocation to high-availability node and a VRE penetration of $2d_{h+l}$ roughly depicts the setting in Schmidt and Zinke (2020).

(2020) consider regional VRE potentials, which limit the capacity allocation to regions with a high average availability. This limitation increases the capacity allocation to nodes with lower average availability under uniform pricing compared to my analysis. Hence, if the authors would ignore limited potentials and allocate all VRE capacities, welfare losses would likely be substantially higher.

The model's simplicity allows to fundamentally understand the effect of crucial system topology parameters on the spatial allocation of VRE, and the inefficiencies arising under uniform pricing. Despite the model's simplicity, I consider main elements which influence the spatial allocation. While the rationales I identify should remain, additional effects may occur when considering a more realistic setting. In the following paragraphs I discuss central simplifications and potential impacts.

I model the spatial allocation decision as a one-shot game in which producers can observe a fixed system topology. Based on this topology, producers allocate capacity between the two nodes. In reality, the parameters of the system topology, such as VRE penetration, transmission capacity and demand distribution, change continuously over time in a dynamic process. If only the VRE capacity increases continuously over time, the three ranges identified can be translated into three phases. Namely, initial VRE capacity is allocated at the high-availability node, then capacity is allocated at the low-availability node, and when a high VRE penetration level is reached, capacity is split between the two nodes. In the more likely case of multiple parameters evolving over time, the optimal spatial allocation becomes much more complex. A still simple example could be a continuous increase in VRE capacity and a discrete transmission capacity at one point in time. In such a case, generators allocating VRE capacity need to consider the proportion of the lifetime of the plant before and after the increase in transmission capacity. A possible outcome could be that in a period with moderate VRE penetration, which is well before the transmission capacity increase, it is optimal to allocate a high proportion of capacity to the low-availability node. As the date of the transmission capacity increase approaches, it would be optimal to increasingly allocate VRE capacity to the high-availability node. In reality, therefore, the three ranges identified are unlikely to translate into three phases of capacity expansion. Nevertheless, the results improve the general understanding of the impact of changes in the system topology on the spatial allocation of VRE.

Second, to ensure an analytical solution and to gain a profound theoretical understanding I do not analyse the effect of storage and demand flexibility in the model. However, storage and demand flexibility represents important elements of the system topology and influence the spatial allocation of VRE. This is because storage and demand flexibility provide means to better align VRE output with demand, by shifting the time

of output provision or shifting the time of demand. The IEA (2022b) assumes storage and demand flexibility to provide a quarter of the required flexibility each in the year 2050 in the Announced Policy Scenario. In my model, storage operators would maximise profits by injecting during periods of high VRE output (i.e., VRE technology sets the price) and withdrawing during periods of low VRE output (i.e., conventional technology sets the price). Similarly, operators of demand flexibility would maximise profits form flexibility when shifting demand from periods with high VRE output to periods with low VRE output. This implies, with increasing storage and demand flexibility the sum of output from VRE and storage minus flexible demand becomes less volatile. This is similar to a decrease in the variance of the availability profile. An increase in flexible capacity should therefore have similar effects like a decrease in the variance, which I analyse in Section 3 and 4. Czock et al. (2022), who analyse the optimal storage allocation find storage to be predominantly built at transmission bottlenecks, such that curtailment before bottlenecks decreases. This corresponds to building storage capacity mainly at the high-availability node in my model. Considering such a spatial allocation of storage would increase in the VRE capacity at the high-availability node for most VRE penetration levels compared to my analysis.

Furthermore, I only consider a two-node network. Considering a complex network with multiple nodes yield output to be transported via multiple nodes. These nodes' remaining available transmission capacity is reduced in such a case. Hence, in case of multiple nodes, not only does the transmission capacity of the producing or importing node affect the spatial allocation of VRE, but also the transmission capacity of all nodes in between.

Furthermore, the analysis only considers one VRE technology and one conventional technology. In most countries, at least two VRE technologies, namely wind and solar, are employed. The coexistence of the VRE technologies likely induces additional interaction effects. For instance, when demand is regionally equally distributed, solar conditions are similar across a country, and wind capacities are located mostly in the north, it would be optimal to allocate more solar capacity to the south than to the north. In contrast, it would be optimal to allocate solar capacity would be predominantly to the north, when most wind capacities are located in the south. Thereby the effects also depend on the penetration level of each VRE technology and the correlation of availabilities among the different VRE technologies. Similar dependencies likely arise from multiple conventional technologies with differing variable costs.

Another simplification is the assumption of constant and inelastic demand. In reality, demand is neither constant nor inelastic. Instead, demand is fluctuating and slightly positively correlated with VRE availability. This is because demand tends to be higher during the day than at night, which is also the case for solar

availability. Demand also tends to be higher in winter than in summer, which is also the case for wind availability. Furthermore, household and industrial electricity demand features some level of price elasticity (Cialani and Mortazavi, 2018). Taking such demand characteristics into account is likely to affect the results in the following way: The *high-availability deployment range* is likely to be valid also for higher VRE penetration levels. First, because curtailments at node h would be lower due to the positive correlation between demand and VRE availabilities. And second, because the remaining curtailments would be partly offset by an increase in elastic demand due to the lower average price level at node h. The *low-availability deployment range* is likely to be narrowed. This is because the range cut-off point is reached when curtailment occurs at node l, and with non-constant demand, low demand may coincide with high VRE availabilities, triggering curtailment. Under *split capacity deployment range*, the share of capacity allocated to the high-availability node is likely to increase if elastic demand is considered. This is because average prices at node h are on average lower than at node l, so the share of demand at node h increases. The increase in demand translates into an increase in electricity prices at node h, which then increases the willingness of investors to allocate capacity to node h.

While the two most common market designs are uniform and nodal pricing, the exact regulation usually differs from the two cases I analyse. A prominent example is the compensation of VRE capacity in case of redispatch under uniform pricing. I assume, like Schmidt and Zinke (2020) and Pechan (2017), curtailed producers of VRE are compensated with the market price. In some countries, like Spain, the compensation of VRE capacity in case of redispatch is below market prices, such that producers consider the curtailments, when deciding on the spatial allocation (Bird et al., 2016). The lower the compensation, the closer the capacity allocation to the one arising under nodal pricing. However, studies that analyse the effects of reduced compensations on spatial allocation are lacking. Such studies would get increasingly relevant as countries, such as the UK, consider reducing their compensations (Cholteeva, 2020).

6. Conclusion

To date, there is a lack of theoretical literature that provides a comprehensive understanding of the implications of VRE allocation. This paper contributes to this research gap by developing a theoretical model that depicts the spatial allocation of VRE in a two-node network. Using the model, I analyse under which conditions it is welfare enhancing to allocate some VRE capacity to locations with unfavourable potential output. Furthermore, I assess how the spatial allocation under uniform pricing differs from the optimum and derive the resulting welfare effects.

From a theoretical perspective, my contribution is threefold: First, I show analytically that the optimal spatial allocation can be grouped into three spatial allocation ranges. Second, I show how the width of each range and the allocation when capacity is split is determined by the different parameters of the system topology. And third, I identify the allocation under uniform pricing and the resulting welfare loss, and show how the welfare loss is affected by the different parameters of the system topology. In addition, my study can assist policymakers when designing policies that affect the spatial allocation, or investors trying to identify the profit-maximising allocation of VRE investments.

I develop a stylised model which provides a fundamental understanding of the dynamics and interactions in the allocation of VRE. However, additional effects are likely to occur when considering a setting with a realistic network, multiple VRE and conventional technologies, as well as storage and demand elasticity. The same holds true when considering endogenous investments not only in VRE but also in additional technologies, such as transmission capacity. Taking into account real-world constraints, such as limited regional VRE potentials, is likely to reduce the inefficiencies observed under uniform pricing.

Further research could extend the model to include additional technologies. For example, investigating a second VRE technology would allow understanding the interdependencies of expanding wind and solar capacity at the same time. The inclusion of elastic demand and storage would allow the analysis of how flexibility affects the spatial distribution of VRE. It could also identify combinations of VRE and storage capacity sufficient to meet all demand with VRE. The implementation of endogenous investments in transmission capacity would make it possible to identify the effects of such investments on the spatial allocation of VRE. This would provide insights into the trade-off between a network-friendly allocation of VRE and the expansion of transmission capacity. Finally, the implementation of a more realistic network would allow to study the impact of curtailments occurring at nodes between production and consumption nodes on the spatial allocation.

Acknowledgements

The author would like to thank Christian Tode and Marc Oliver Bettzüge for their thoughtful and constructive comments and discussions on this work. Additionally, I would like to thank Berit Czock and Felix Schäfer for their helpful comments. The paper also benefited from discussions at the 29$^{\text{th}}$ YEEES Seminar 2022 in Ghent. The author conducted this work in the Hans-Ertel-Centre for Weather Research framework, funded by the German Federal Ministry for Digital and Transport (grant number BMVI/DWD 4818DWDP5A). The content of this paper reflects the opinions of its author only and not those of EWI.

Appendix A. Historical availabilities for wind and solar in Germany and corresponding Beta distribution

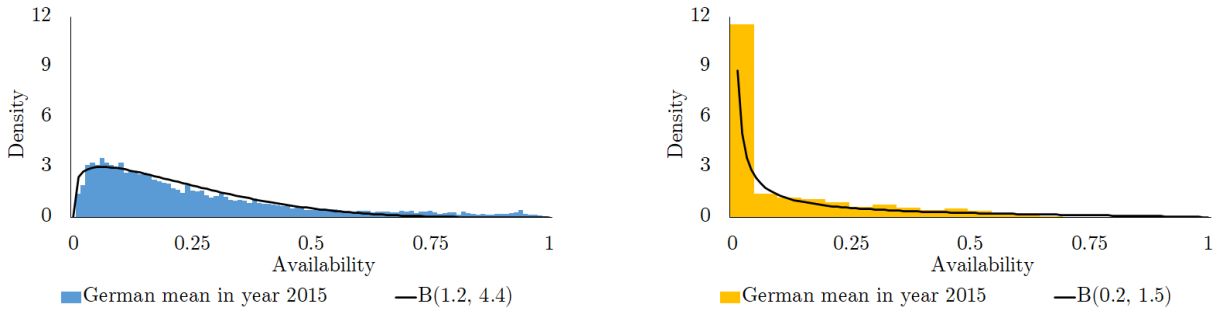

(a) Wind Onshore (b) Solar

Figure A.14: Comparison of historical availabilities for wind and solar in Germany with the corresponding Beta distribution.

Appendix B. Applied and historical densities for wind power

Figure B.15 shows the density of potential output assumed for the high and low-availability node in all figures of Section 3 and 4 with constant availability distribution parameters (i.e., Figure 2, 3, 4, 5, 9, 10, 11). Additionally, the Figure B.15 displays the density of estimated historical wind power availabilities for the year 2015-2022 in the German market areas TransnetBW and Tennet. The estimation is based on data from the Bundesnetzagentur's electricity market information platform (BNetzA, 2022). TransnetBW is located in the south of Germany, and most wind power plants in the Tennet market area are located in the north. This implies that the availability density parameters in the analysis at hand resemble the availabilities for wind in the north (h) and south (l) of Germany.

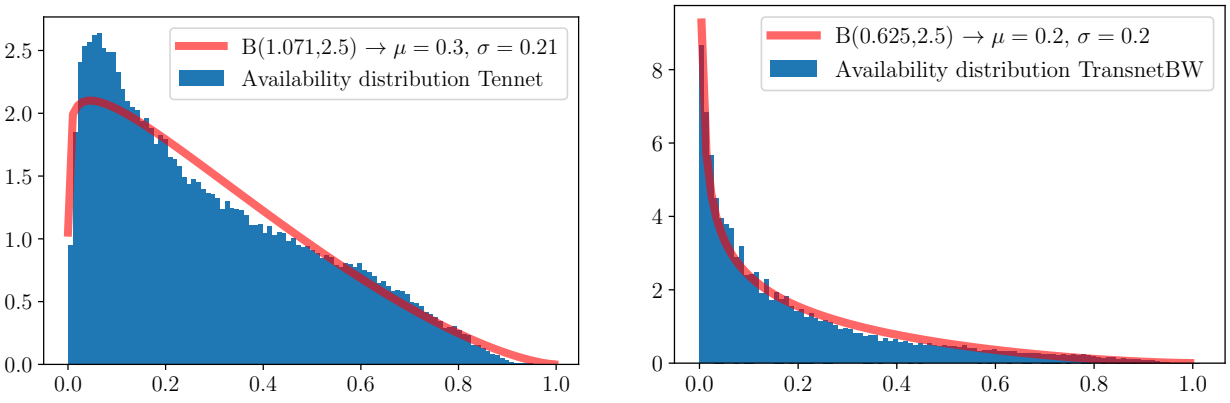

(a) High-availability node (b) Low-availability node

Figure B.15: Historical availability densities for the years 2015-2022 and in this analysis applied densities.

Appendix C. Effect of changing μ_i with the means of α_i on σ_i

The Beta distribution $B(\alpha, \beta)$is defined by the parameter α and β. These parameters define the average and the standard deviation. When changing the average with the means of changing α. The standard deviation remains rather constant.

Figure C.16a) shows the effect of varying μ_i in the interval [0.2,0.5] with the means of changing α_i for the case of $\beta = 4.4$. The density function and the resulting standard deviation are displayed. One can see that the density functions moves, while standard deviation remains rather constant, varying only between 0.2 and 0.22.

Figure C.16b) displays the maximum change in the standard deviation when varying α_i, such that μ_i is varied in the interval [0.2,0.5] for different level of β. One can see, that the maximum change in the variance for $\beta \in [0.5, 40]$ does not exceed 0.04. For $\beta > 2.2$ the maximum change does not exceed 0.02.

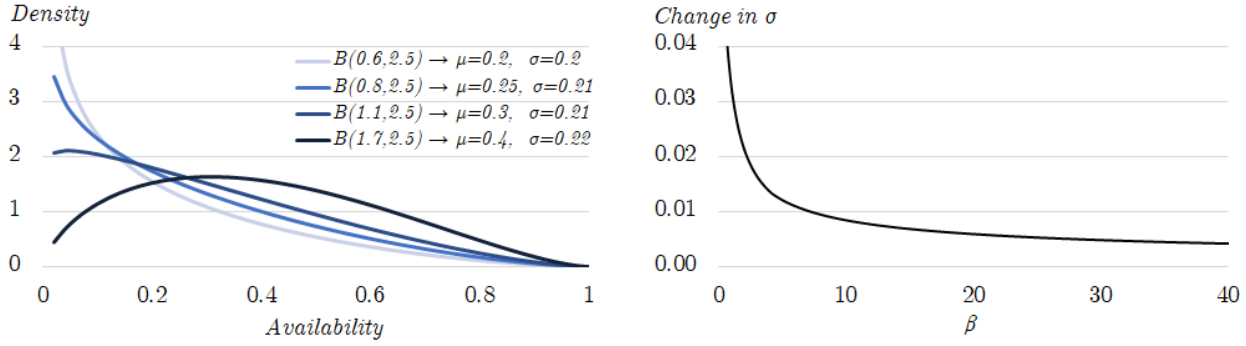

(a) Effect on density

(b) Effect on σ when varying $\mu \in [0.2, 0.5]$

Figure C.16: Effect on σ when changing μ with the means of α.

Appendix D. Effects of the variance on the spatial allocation ranges when transmission capacity is high

Figure D.17 displays the insights from Finding NP 7 numerically for the case of high transmission capacity (i.e., $t = \frac{3}{4}d_i$). Assumptions regarding the demand and the availability profiles are identical to Figure 6.

When the variance is increased at node h (compare Figure D.17a and b), the *high-potential deployment range* is shortened from $2.0d_{h+l}$ to $1.4d_{h+l}$. Additionally, the figure confirms that increasing σ_i^2 lowers the nodal capacity share in the *split capacity range* independent of the VRE penetration level.

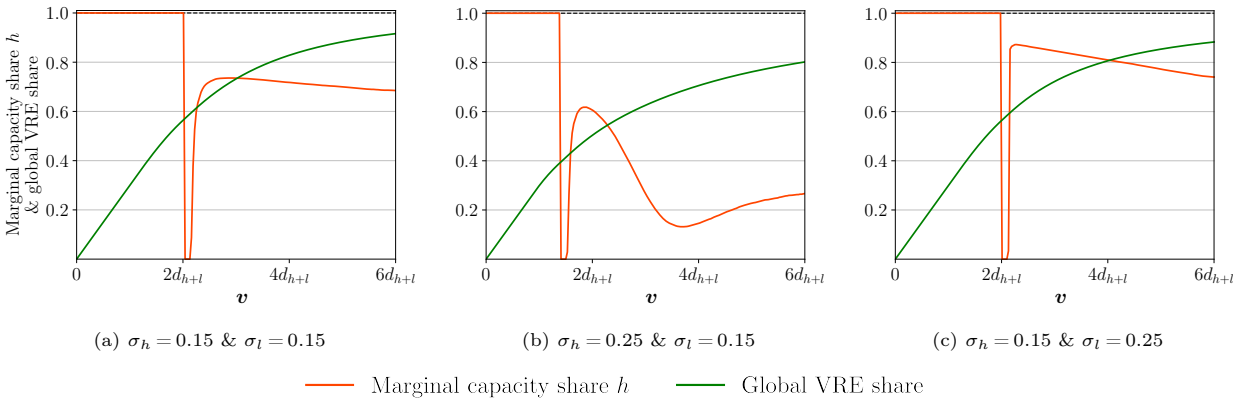

(a) $\sigma_h = 0.15$ & $\sigma_l = 0.15$ (b) $\sigma_h = 0.25$ & $\sigma_l = 0.15$ (c) $\sigma_h = 0.15$ & $\sigma_l = 0.25$

Figure D.17: Effect of the variance in the availability profile on the spatial allocation ranges under nodal pricing.

References

ACER, 2022. Decision No 11/2022 of the European Union Agency for the Cooperation of Energy Regulators of 8 August 2022 on the alternative bidding zone configurations to be considered in the bidding zone review process. URL: https://www.acer.europa.eu/sites/default/files/documents/Individual%20Decisions/ACER%20Decision%2011-2022%20on%20alternative%20BZ%20configurations.pdf.

Bird, L., Lew, D., Milligan, M., Carlini, E.M., Estanqueiro, A., Flynn, D., Gomez-Lazaro, E., Holttinen, H., Menemenlis, N., Orths, A., Eriksen, P.B., Smith, J.C., Soder, L., Sorensen, P., Altiparmakis, A., Yasuda, Y., Miller, J., 2016. Wind and solar energy curtailment: A review of international experience. Renewable and Sustainable Energy Reviews 65, 577–586. doi:10.1016/j.rser.2016.06.082.

BNetzA, 2022. SMARD - Electricity market data for Germany. URL: https://www.smard.de/en.

Cholteeva, Y., 2020. Constraint payments: rewarding wind farms for switching off. URL: https://www.power-technology.com/features/constraint-payments-rewarding-wind-farms-for-switching-off/.

Cialani, C., Mortazavi, R., 2018. Household and industrial electricity demand in Europe. Energy Policy 122, 592–600. URL: https://www.sciencedirect.com/science/article/pii/S0301421518305068, doi:10.1016/j.enpol.2018.07.060.

Czock, B., Sitzmann, A., Zinke, J., 2022. The place beyond the lines - Efficient storage allocation in a spatially unbalanced power system with a high share of renewables, display, Bonn. URL: https://meetingorganizer.copernicus.org/EMS2022/EMS2022-196.html, doi:10.5194/ems2022-196.

Elberg, C., Hagspiel, S., 2015. Spatial dependencies of wind power and interrelations with spot price dynamics. European Journal of Operational Research 241, 260–272. URL: https://linkinghub.elsevier.com/retrieve/pii/S0377221714006614, doi:10.1016/j.ejor.2014.08.026.

Fürsch, M., Hagspiel, S., Jägemann, C., Nagl, S., Lindenberger, D., Tröster, E., 2013. The role of grid extensions in a cost-efficient transformation of the European electricity system until 2050. Applied Energy 104, 642–652. URL: https://linkinghub.elsevier.com/retrieve/pii/S0306261912008537, doi:10.1016/j.apenergy.2012.11.050.

Green, R., 2007. Nodal pricing of electricity: how much does it cost to get it wrong? Journal of Regulatory Economics 31, 125–149. URL: http://link.springer.com/10.1007/s11149-006-9019-3, doi:10.1007/s11149-006-9019-3.

IEA, 2022a. VRE share in annual electricity generation in selected countries, 2016-2022. URL: https://www.iea.org/data-and-statistics/charts/

vre-share-in-annual-electricity-generation-in-selected-countries-2016-2022.

IEA, 2022b. World Energy Outlook 2022. Paris.

Kies, A., Schyska, B., von Bremen, L., 2016. Curtailment in a Highly Renewable Power System and Its Effect on Capacity Factors. Energies 9, 510. URL: http://www.mdpi.com/1996-1073/9/7/510, doi:10.3390/en9070510.

Müller, T., 2017. The Role of Demand Side Management for the System Integration of Renewable Energies, in: IEEE. doi:10.1109/EEM.2017.7981892.

Obermüller, F., 2017. Build wind capacities at windy locations? Assessment of system optimal wind locations , 31.

Pechan, A., 2017. Where do all the windmills go? Influence of the institutional setting on the spatial distribution of renewable energy installation. Energy Economics 65, 75–86. URL: https://linkinghub.elsevier.com/retrieve/pii/S0140988317301457, doi:10.1016/j.eneco.2017.04.034.

Schmidt, L., Zinke, J., 2020. One price fits all? Wind power expansion under uniform and nodal pricing in Germany 20, 44.

Schweppe, F.C., Caramanis, M.C., Tabors, R.D., Bohn, R.E., 1988. Spot Pricing of Electricity. Springer US, Boston, MA. URL: http://link.springer.com/10.1007/978-1-4613-1683-1, doi:10.1007/978-1-4613-1683-1.

Sinden, G., 2007. Characteristics of the UK wind resource: Long-term patterns and relationship to electricity demand. Energy Policy 35, 112–127. URL: https://linkinghub.elsevier.com/retrieve/pii/S0301421505002752, doi:10.1016/j.enpol.2005.10.003.

Sinn, H.W., 2017. Buffering volatility: A study on the limits of Germany's energy revolution. European Economic Review 99, 130–150. URL: https://linkinghub.elsevier.com/retrieve/pii/S0014292117300995, doi:10.1016/j.euroecorev.2017.05.007.

Staffell, I., Pfenninger, S., 2016. Using bias-corrected reanalysis to simulate current and future wind power output. Energy 114, 1224–1239. URL: https://linkinghub.elsevier.com/retrieve/pii/S0360544216311811, doi:10.1016/j.energy.2016.08.068.

Yasuda, Y., Bird, L., Carlini, E.M., Eriksen, P.B., Estanqueiro, A., Flynn, D., Fraile, D., Gómez Lázaro, E., Martín-Martínez, S., Hayashi, D., Holttinen, H., Lew, D., McCam, J., Menemenlis, N., Miranda, R., Orths, A., Smith, J.C., Taibi, E., Vrana, T.K., 2022. C-E (curtailment – Energy share) map: An objective and quantitative measure to evaluate wind and solar curtailment. Renewable and Sustainable Energy Reviews 160, 112212. URL: https://linkinghub.elsevier.com/retrieve/pii/S1364032122001356,

doi:10.1016/j.rser.2022.112212.

Zerrahn, A., Schill, W.P., Kemfert, C., 2018. On the economics of electrical storage for variable renewable energy sources. European Economic Review 108, 259–279. URL: https://linkinghub.elsevier.com/retrieve/pii/S0014292118301107, doi:10.1016/j.euroecorev.2018.07.004.